First observation of the dynamics of nano-scale particulates in diesel exhaust via small-angle x-ray scattering (SAXS).

Gregory Beaucage (UC), Patrick Kirchen (ETHZ), T. Narayanan (ESRF), Konstantinos Boulouchos (ETHZ).
UC (University of Cincinnati, Cincinnati OH USA), ESRF (European Synchrotron Research Facility, Grenoble, France) and ETHZ (Eidgenössische Technische Hochschule Zürich, Zürich, Switzerland)

In order to reduce emissions of nano-scale particulates in engine exhaust streams it is important to understand the mechanisms of formation and growth of nano-particulates. The structure of nano-scale particles may be modified by sampling techniques such as dilution or in filters making in situ measurements more useful. Further, observation of the dynamics of nano-particle structural changes as a function of engine conditions during acceleration and deceleration, start-up/shut-down or under variable load are most useful if real time data is available. Despite a wide range of analytic measures of nano-scale soot, a direct, non-destructive observation in engine exhaust streams is of interest to understanding and removal of this potentially dangerous combustion byproduct [1-10].

We have recently developed for the first time an in situ technique using x-ray scattering (SAXS) at synchrotron facilities that can directly quantify the nano-particle size distribution, the particle number density and volume fraction as well as simultaneously measuring the details of aggregate/agglomerate structure in terms of the aggregate radius of gyration, mass fractal dimension and quantitative measures of the branch content and polydispersity of aggregates [11-21]. SAXS can distinguish between aggregate and primary particle structure in 20 ms measurements on dilute aerosol streams allowing for resolution of transient structural signatures. Here, the first application of this analytic technique to in situ studies of exhaust stream is described [22]. A small portable diesel engine used in an electric generator is used.

We have investigated nano-particulate structural changes during start-up, acceleration, deceleration and under variable load. For example, Figure 1 shows typical in situ scattering data, x-ray intensity versus scattering vector or reduced angle. From the fit to the data using the unified function [13,15,17-19] we can determine the particle size distribution curves shown as an inset in Figure 1. Only the nucleation mode particle size distribution is shown, though the accumulation mode is also measured. The number and volume distributions are shown. We can also determine details of the aggregate/agglomerate structure. Figure 1b shows the experimental setup with the diesel generator in the foreground and the x-ray beam passing horizonal through the tube near Patrick Kirchen. The exhaust stream passes vertically near Pat's hands.

Figure 2 shows some of the parameters from a fit to such a scattering curve mapped as a function of time during dynamic deceleration of the diesel engine. In Fig. 2a the Sauter mean diameter (and radius of gyration for the nano-particles in the nucleation mode) is seen to decrease on deceleration at about 12 s. This coincides with a rise in the number density, Fig. 2b, under almost constant nano-particulate volume fraction. Aggregates of nanoparticles, accumulation mode, also decrease in size on deceleration from a size scale beyond the large limit of the scattering geometry at short times. The mass fractal dimension decreases on deceleration making looser aggregates/agglomerates. Aggregates are polydisperse and this polydispersity can be quantified in this measurement.

We hope to extend these initial in situ quantifications of the dynamics of nano-particle growth under variable engine conditions, fuel additives, fuel types and exhaust treatment systems and as a function of residence time (position) in the exhaust stream.

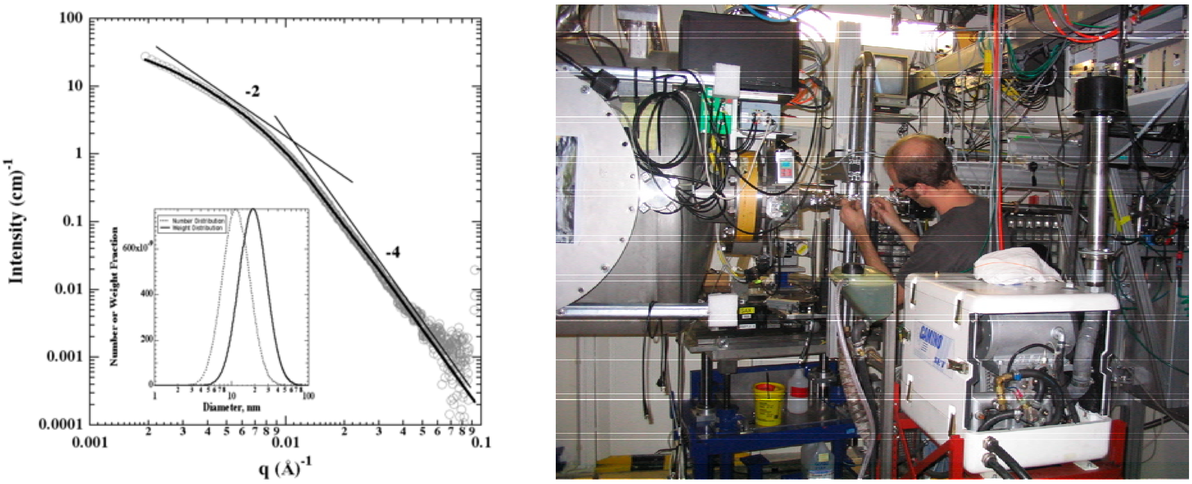

a) b)

Figure 1. a) In situ SAXS from measurements for diesel exhaust at ESRF in France. Scattered intensity is plotted against scattering vector (reduced angle). The fit is to the unified function developed by Beaucage [17-19]. Inset shows particle size distribution obtained from the high-q part of this data set. PDI (below) for this particle size distribution is about 6.4. d_p = 19.2 nm; σ_g = 1.48 (PDI = 6.40), d_f = 2.10, c= 1.03, z = 43.6, $)_{Br}$ = 0.104. b) Pat Kirchen adjusting the in situ SAXS measurement at ESRF. X-ray beam passes from right to left through the horizontal tube to Pat's left. Diesel generator is seen in the foreground. Exhaust tube passes vertically near Pat's hands.

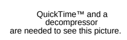

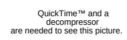

a) b)

Figure 2. Diesel exhaust measurements at ESRF in France with an engine from ETHZ. Measurement is made during deceleration of the engine from high load at about 12 s. Measurements are made at 3/s though a rate of 50/s is possible. a) Nano-soot particle size versus time with point of deceleration shown by a vertical line. d_p is the Sauter mean nano-particle diameter, R_{g1} is the nanoparticle radius of gyration, PDI is a unitless measure of the particle size distribution with 1 being monodisperse, R_{g2} is the radius of gyration of aggregates of the nano-soot (aggregates are larger than the measurement size before deceleration) and d_f is the mass fractal dimension for these aggregates. b) Nano-particle number density, N, and volume fraction V_f as a function of time with point of deceleration shown by the vertical line.

1) *Engines and Nanoparticles: A Review.* Kittelson DB, *J. Aerosol Sci.* **29** 575-588 (1998).
2) *Comparison study of particle measurements systems for future type approval application. Report 202770 Eidgenossische Materialprufungs-und Forschungsanstalt (EMPA) Dubendorf Switzerland*, (*www.empa.ch/plugin/template/empa/*/20988/---/=1*) Mohr M, Lehmann U (2003).
3) *Physical characterization of particulate emissions from diesel engines: a review.* Burtscher H *Journal of Aerosol Science* **36** 896-932 (2005).
4) *PM measurement artifact: organic vapor deposition on different filter media.* Chase RE, Duszkiewicz GJ, Richert JFO, Lewis D, Maricq MM, Xu N *SAE 2004-01-967* (2004).
5) *Continuous PM-10 measurement using the tapered element oscillating microbalance.* Patashnick H, Rupprecht EG *Journal of the Air and Waste Management Association* **41** 1079-1083 (1991).
6) *Quantitative interpretation of divergence between PM10 and PM2.5 mass measurement by TEOM and gravimetric (Partisol) instruments*. Charron A, Harrison RM, Moorcroft S, Booker J *Atmospheric Environment* **38** 415-423 (2004).
7) *Comparison of an alternative particulate mass measurement with advancec microbalance analysis.* Akard M, Oestergaard K, Chase RE, Richert JO, Fukushima H, Adachi M *SAE 2004-01-0589* (2004).
8) *Optical multiwavelength technique applied to the on-line measurement of particle emissions from engines.* Zahoransky RA, Saier T, Laile E, Nikitidis M, Konstandopoulos A *SAE 2001-01-047* (2001).
9) *A closure study of aerosol mass concentration measurements: comparison of values obtained with filters and by direct measurements of mass distributions*. Park K, Kittelson DB, McMurry PH *Atmospheric Environment* **37** 1223-1230 (2003).

10) *Structural properties of diesel exhaust particles measured by transmission electron mictoscopy (TEM): relationships to particle mass and mobility.* Park K, Kittelson DB, McMurry PM *Aerosol Science and Technology* **38** 881-889 (2004).
11) *Probing the dynamics of nanoparticle growth in a flame using synchrotron radiation.* Beaucage G, Kammler HK, Mueller R, Strobel R, Agashe N, Pratsinis SE and Narayanan T, *Nature Mater.* **3,** 370-373 (2004).
12) *In situ studies of nano-particle growth dynamics in premixed flames.* Kammler HK, Beaucage G, Kohls DJ, Agashe N. Ilavsky J., *J Appl. Phys.* **97**(5) 2005 (Article 054309).
13) *Particle size distributions from small-angle scattering using global scattering functions.* Beaucage G, Kammler HK, Pratsinis SE, *J. Appl. Cryst.* **37**, 523-535 (2004).
14) *Structure of flame-made silica nanoparticles by ultra-small-angle X-ray scattering.* Kammler HK, Beaucage G, Mueller R, and Pratsinis SE, *Langmuir* **20**, 1915-1921 (2004).
15) *Determination of branch fraction and minimum dimension of mass-fractal aggregates.* Beaucage G, *Phys. Rev. E*, **70**, 031401 (2004).
16) *In situ crystalline and nano-structural growth kinetics for flame synthesis of titania.* Beaucage G, Londono D, Diemer B, *Chem. Mat.* Submitted (2006).
17) *Approximations leading to a unified exponential/power-law approach to small-angle scattering.* Beaucage G, *J. Appl. Crystallogr.* **28**, 717-728 (1995).
18) *Small-Angle Scattering from Polymeric Mass Fractals of Arbitrary Mass-Fractal Dimension.* Beaucage G, *J. Appl. Crystallogr.* **29**, 134-146 (1996).
19) *Fractal analysis of flame-synthesized nanostructured silica and titania powders using small-angle X-ray scattering*. Hyeon-Lee J, Beaucage G, Pratsinis SE *Langmuir* **14**(20), 5751-5756 (1998).
20) *Non-agglomerated dry silica nanoparticles.* Mueller R, Kammler HK, Pratsinis SE, Vital A, Beaucage G, Burtscher P *Powder Tech.* **140** (1-2): 40-48 (2004).
21) *The effect of external electric fields during flame synthesis of titania*. Kammler HK, Jossen R, Morrison PW, Pratsinis SE, Beaucage G *Powder Tech.* **135**, 310-320 Sp. Iss. SI (2003).
22) *Dynamics of nano-scale particulates in diesel exhaust via small-angle x-ray scattering (SAXS).* Beaucage G, Kirchen P, Boulouchos K, In preparation (2008).

Dynamics of Nanoscale Soot in Diesel Exhaust via Small-Angle X-ray Scattering

Greg Beaucage[a], Pat Kirchen[b], Konstantinos Boulouchos[b], T. Naryanan[c]

[a]Dept. of Chemical and Materials Engineering, University of Cincinnati, Cincinnati, Ohio, USA

gbeaucage@gmail.com; beaucag@uc.edu

[b]Aerothermochemistry and Combustion Systems Laboratory ETH Zurich, Zurich, Switzerland

[c]European Synchrotron Radiation Facility (ESRF), Grenoble, France

12'th ETH Conference on Combustion Generated Nanoparticles

Background: Diffusion Flame Measured at ESRF Grenoble, France

SAXS (Small-Angle X-ray Scattering) for Diesel Exhaust

Why you might be interested in SAXS:

-In situ observation of soot & inorganic nanostructure with no dilution
(calibrate/verify DMA)
-Measure from ~ 1 Å to 1 μm (direct observation of all possible nucleation modes)
-Wide sample concentration range solid powder to exhaust aerosol
-Volatile, semi-volatile, and solid particles (no dilution, charging or denuding)
-Unique details of aggregate structure including mass fractal dimension, branch content
-Volume and number density as well as primary particle size distribution
-20 ms measurement (possibility of observation within engine cycle)

Why you might *not* be interested in SAXS

-Requires a synchrotron for in situ aerosol measurements
(powders can be measured in the lab)
-Non-portable measurement
-More or less requires a specialist (involved data anaylsis)
-Composition is more difficult than structure (electron density or use anomalous SAXS)
-New method (This is the pioneering study and is still in preparation for publication)

Outline

1) SAXS Tutorial - 6 min

2) In situ Flame Work - 2 min

3) In Situ Diesel Exhaust Study - 5 min

4) Summary - 1 min

Background: ESRF Synchrotron Grenoble France

What is SAXS
(Small Angle X-ray Scattering)?

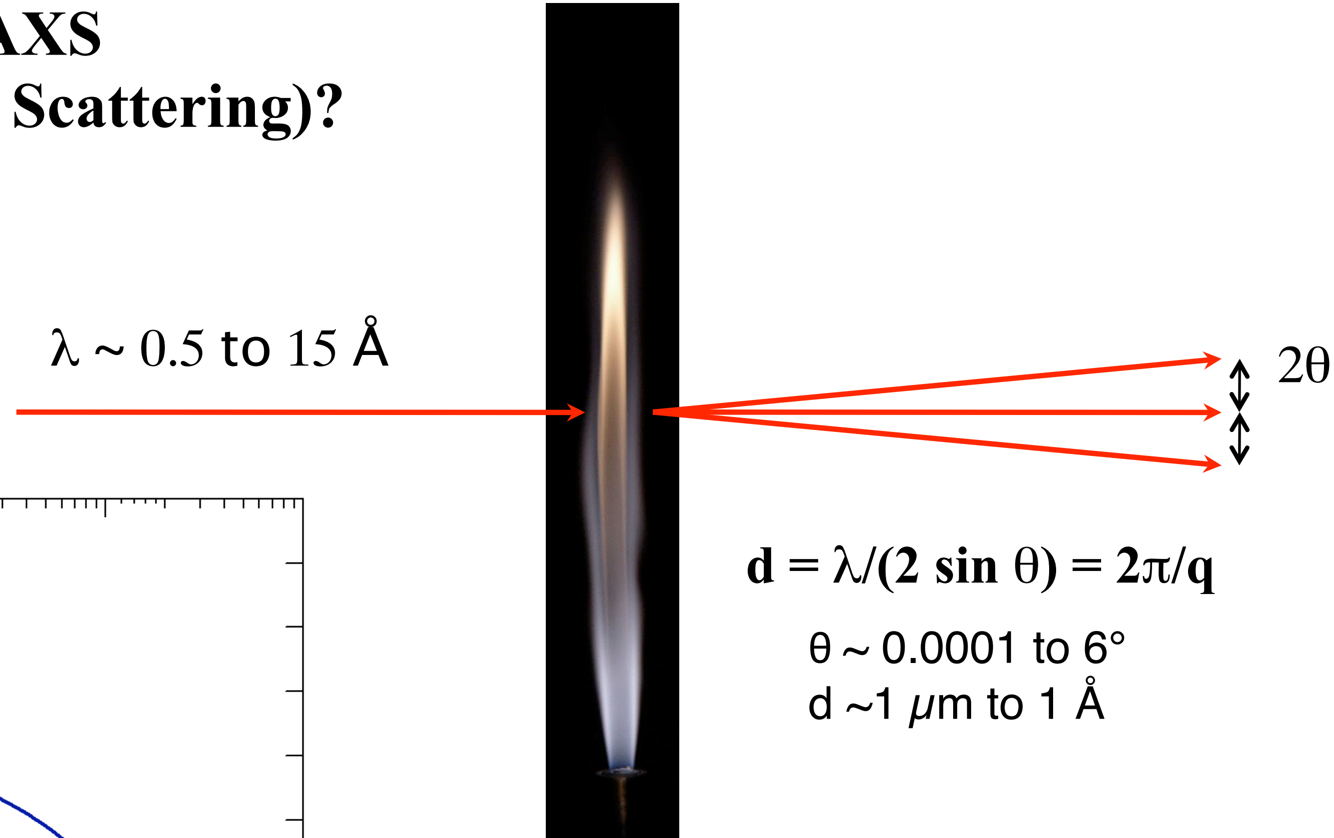

$$d = \lambda/(2 \sin \theta) = 2\pi/q$$

θ ~ 0.0001 to 6°
d ~1 μm to 1 Å

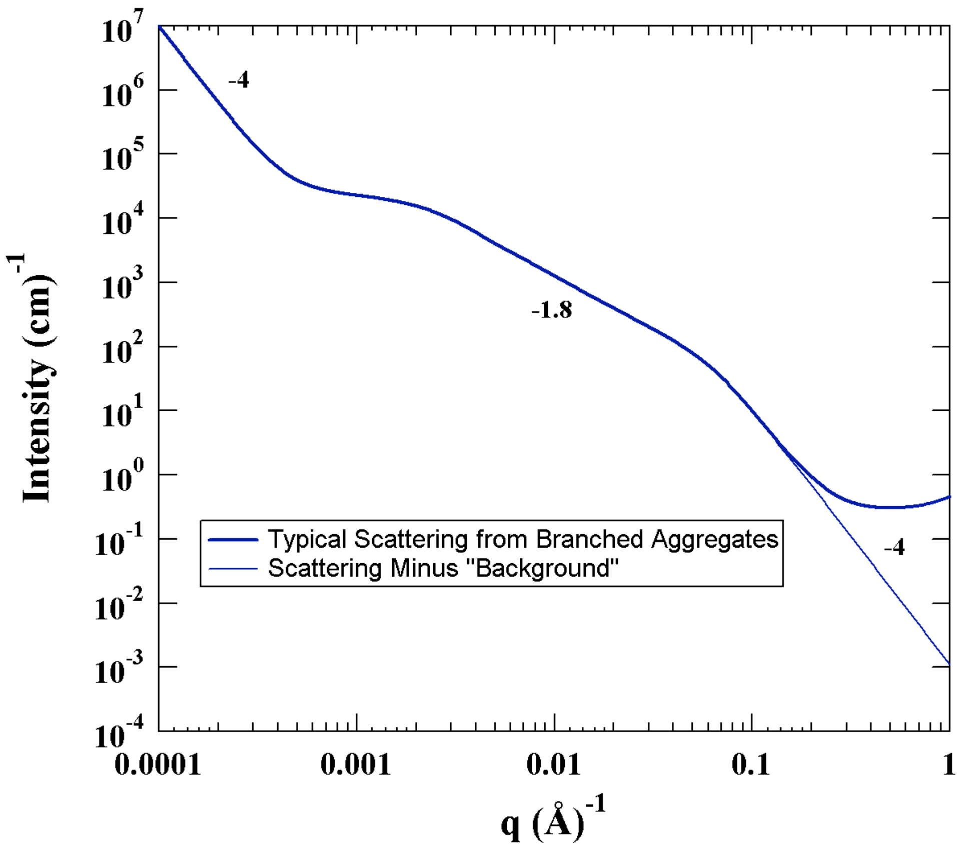

Branched Aggregates

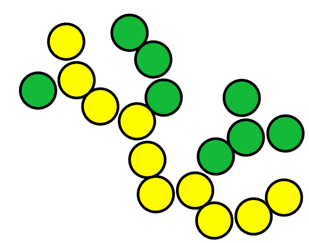

$$q = \frac{2\pi}{d} \qquad I(q) = N(d)\,n_e^2(d)$$

N = Number Density at Size "d"
n_e = Number of Electrons in "d" Particles

Two SAXS Camera Geometries

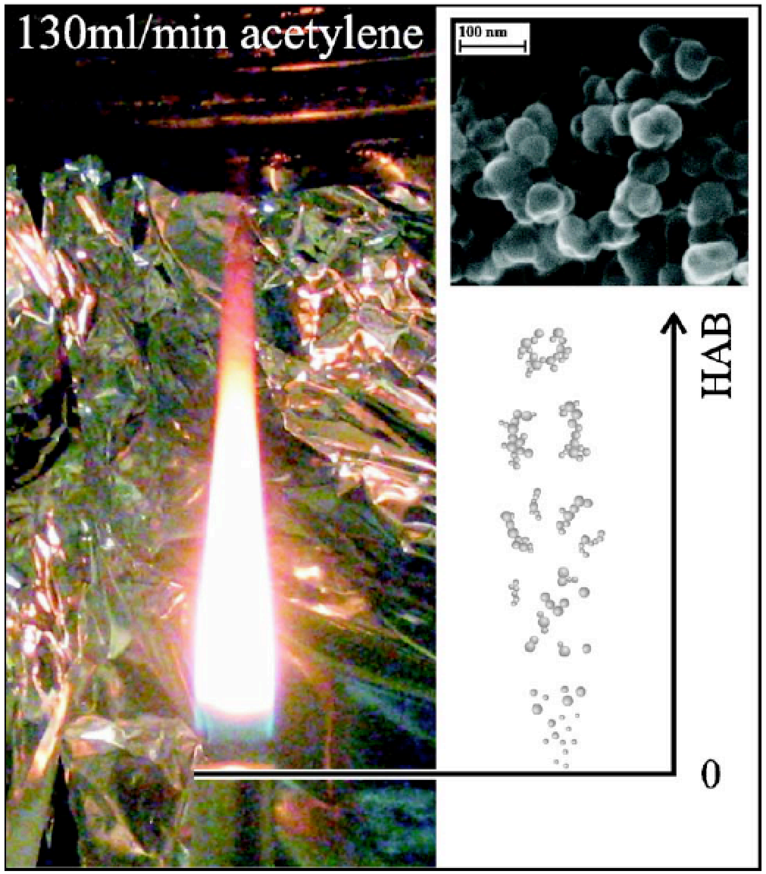

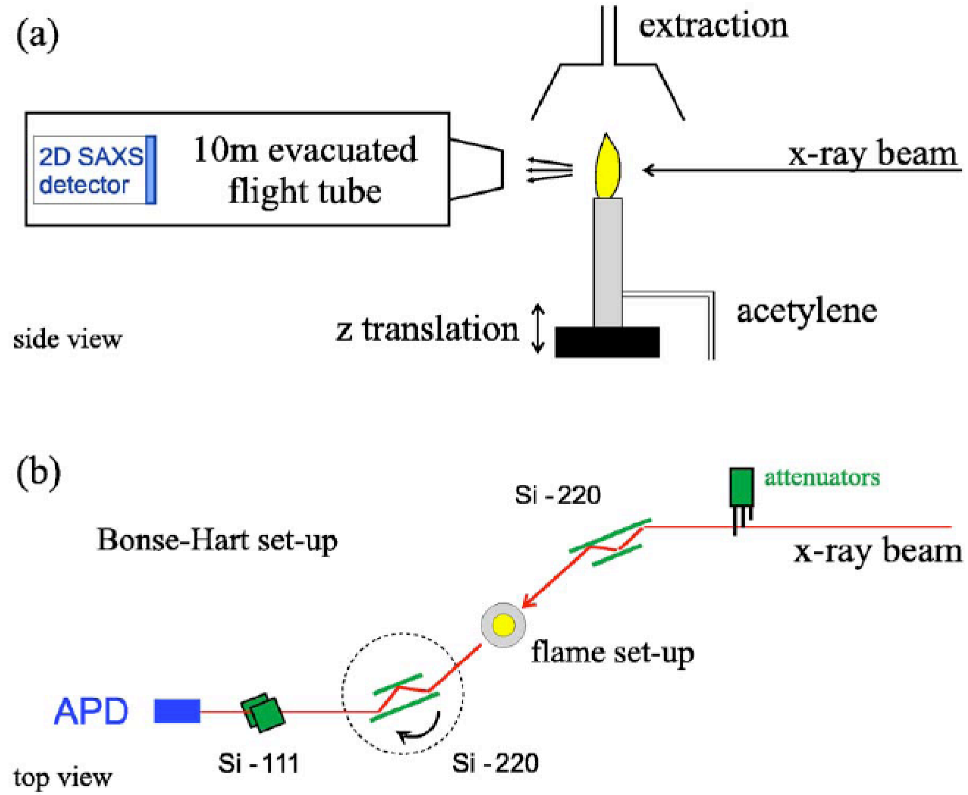

Sztucki M, Narayanan T, Beaucage G, *In situ study of aggregation of soot particles in an acetylene flame by small-angle x-ray scattering* J. Appl. Phys. **101**, 114303 (2007).

Complex Scattering Pattern
(Unified Function, Beaucage 1995 *J. Appl. Cryst.*)

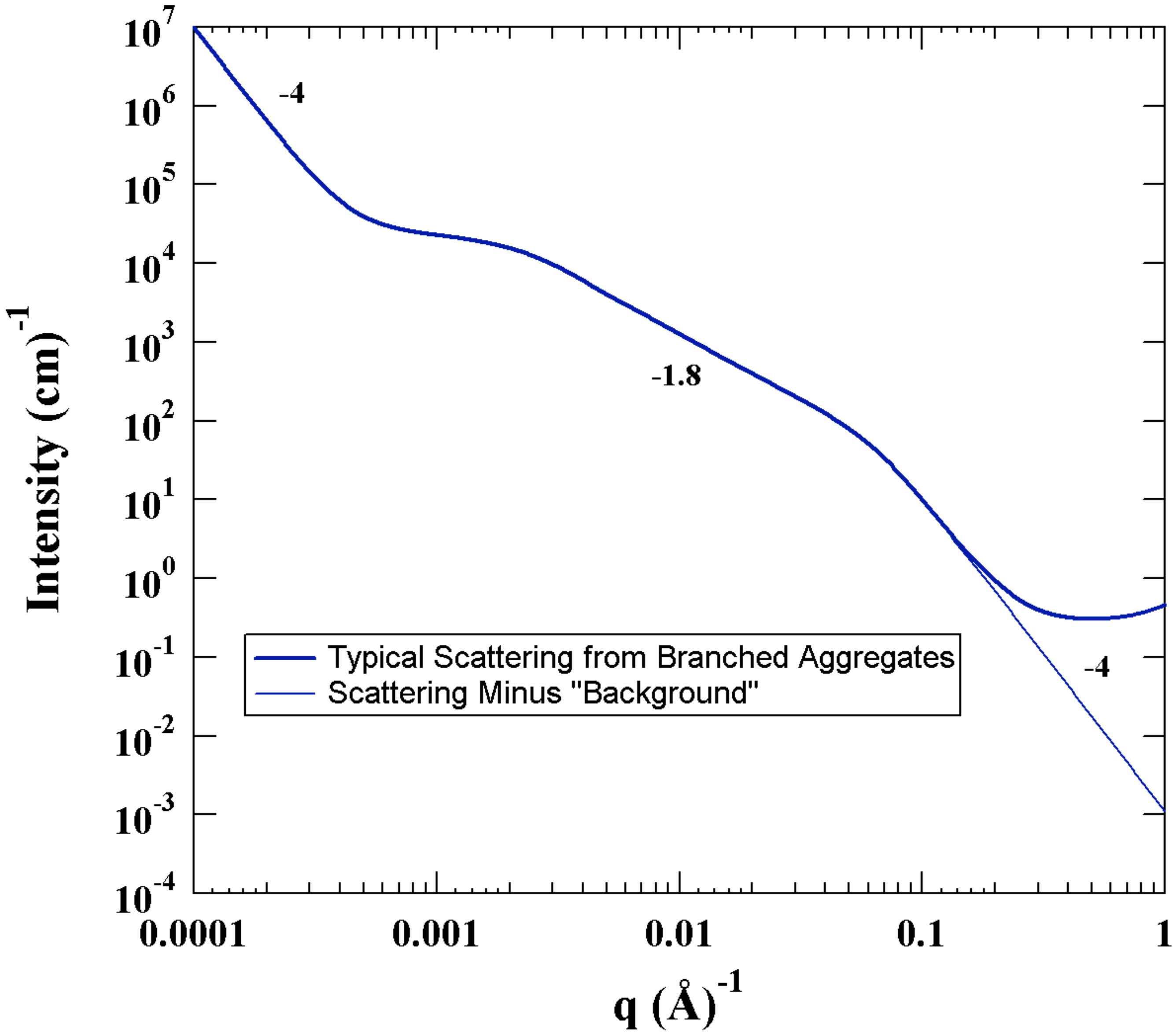

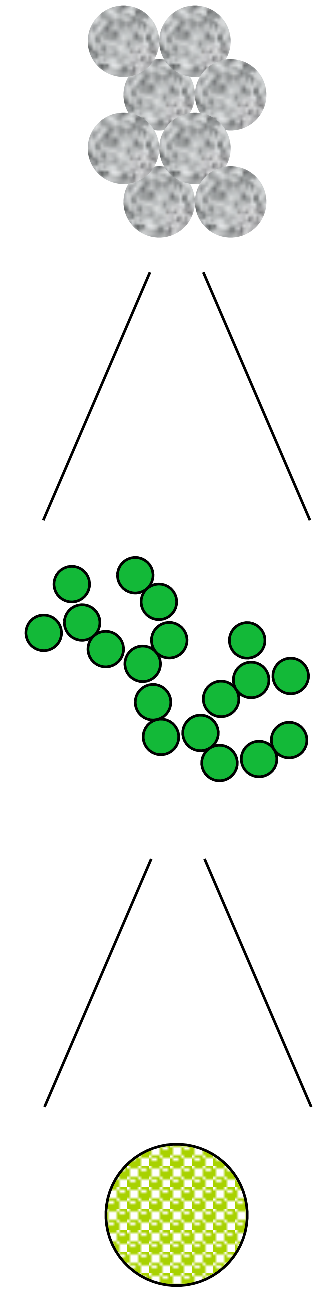

$$q = \frac{2\pi}{d}$$

$$I(q) = N(d)\,n_e^2(d)$$

N = Number Density at Size "d"
n_e = Number of Electrons in "d" Particles

Guinier's Law

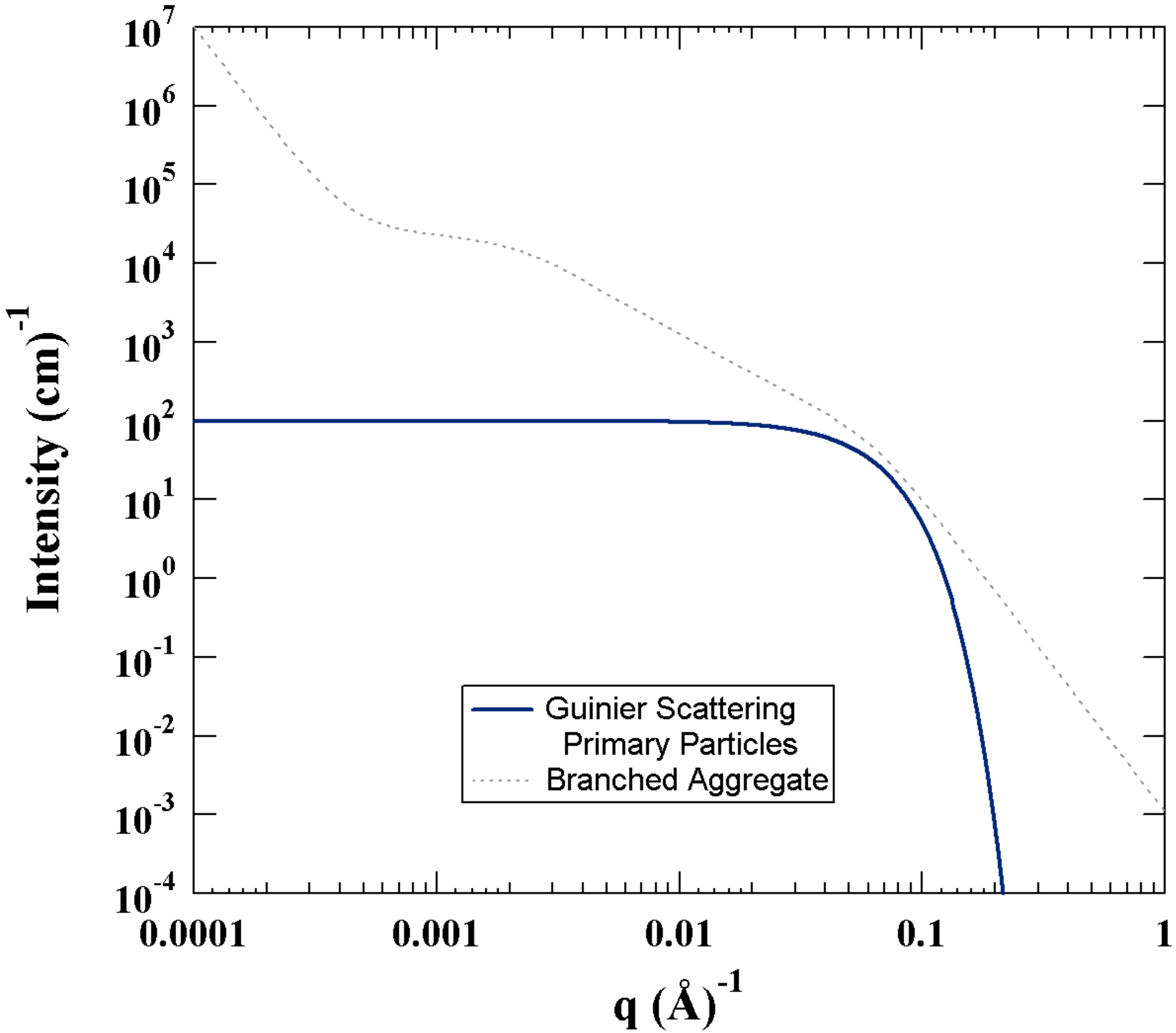

Particle with No Interface

$$I(q) = N(d)n_e^2(d)$$

$$I(q) = G_1 \exp\left(\frac{-q^2\left\langle R_{g,1}^2\right\rangle}{3}\right)$$

$$G = N\rho_e^2\left\langle V^2\right\rangle \sim \left\langle \mathrm{R}^6\right\rangle$$

$$\left\langle R_g^2\right\rangle \sim \frac{\left\langle \mathrm{R}^8\right\rangle}{\left\langle \mathrm{R}^6\right\rangle}$$

Guinier and Porod Scattering

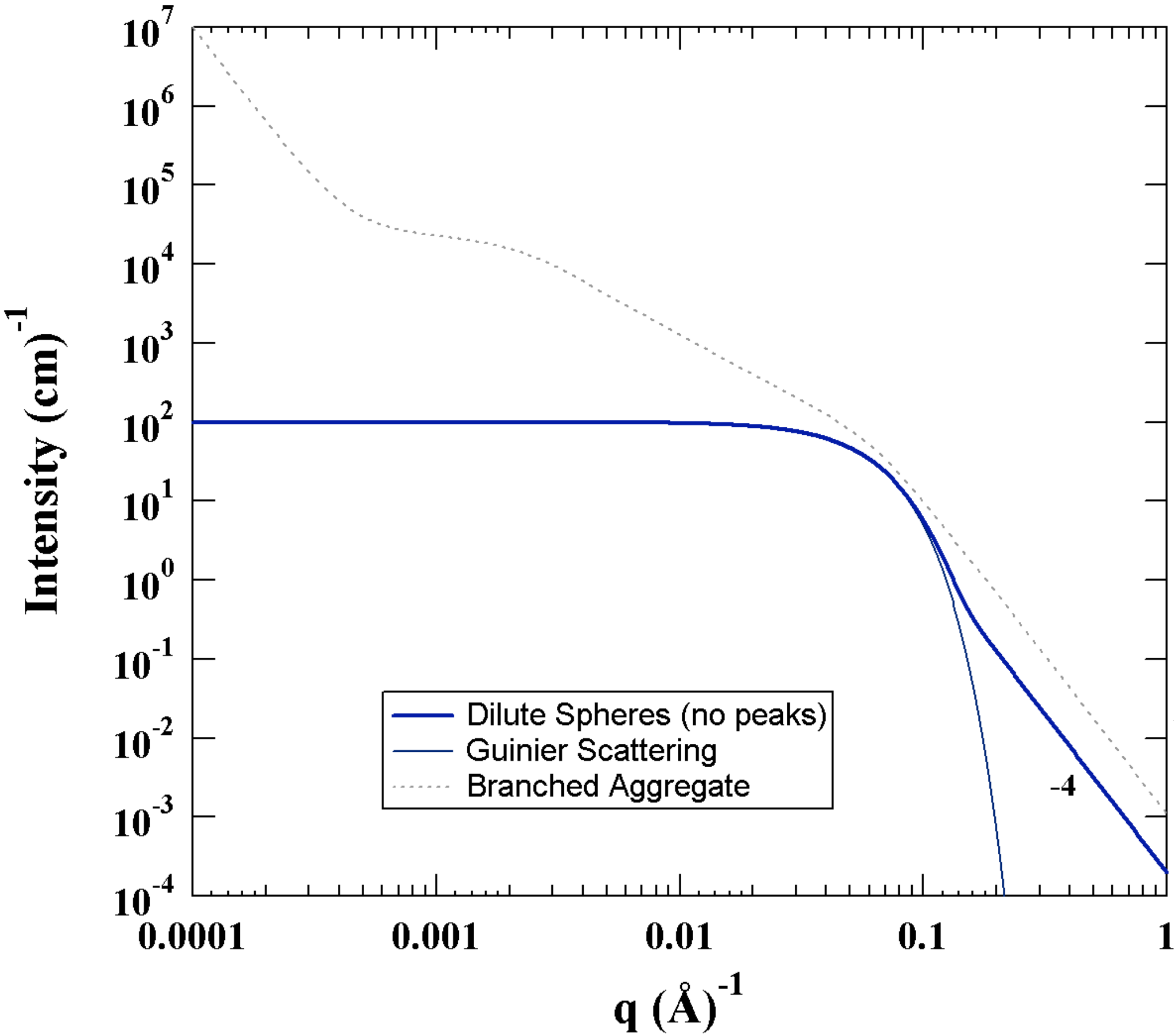

Spherical, Monodisperse Particle With Interface (Porod)

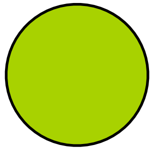

$$I(q) = B_P q^{-4}$$

$$B_P = 2\pi N \rho_e^2 \langle S \rangle$$

$$\langle S \rangle \sim \langle R^2 \rangle$$

$$Q = \int q^2 I(q) dq = N \rho_e^2 \langle R^3 \rangle$$

$$d_p = \frac{Q}{2\pi B_P} = \frac{\langle R^3 \rangle}{\langle R^2 \rangle}$$

Structure of Flame Made Silica Nanoparticles
By Ultra-Small-Angle X-ray Scattering
Kammler/Beaucage Langmuir 2004 20 1915-1921

Polydispersity Index, PDI

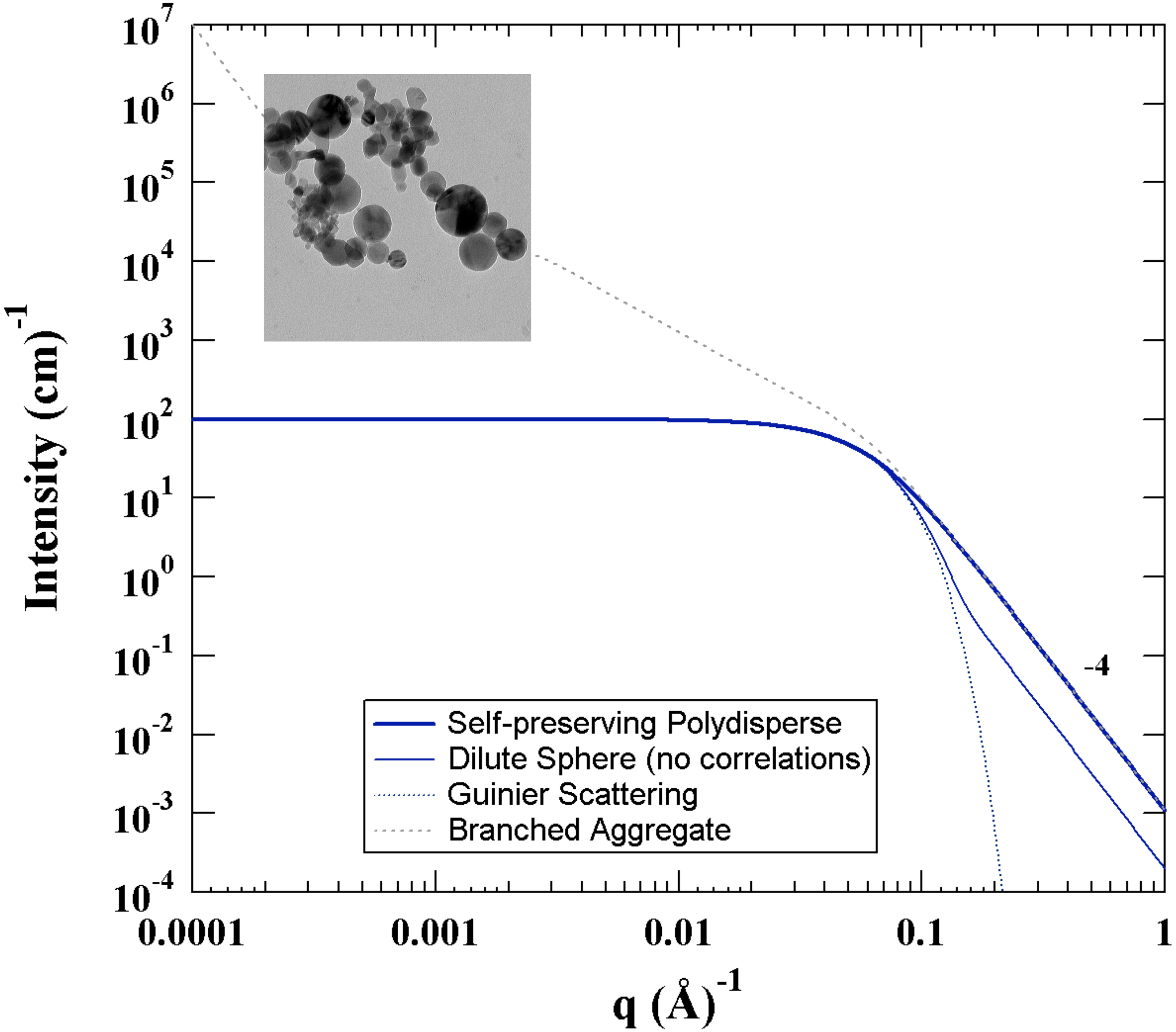

Polydisperse Particles

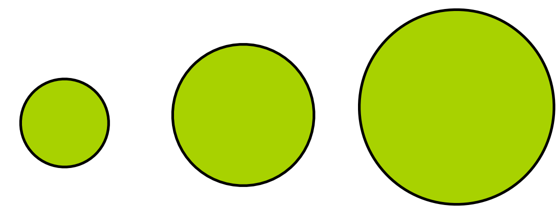

$$PDI = \frac{B_P R_g^4}{1.62G}$$

$$\sigma = \ln(\sigma_g) = \left[\frac{\ln(PDI)}{12}\right]^{1/2}$$

$$m = \left[\frac{5R_g^2}{3e^{14\sigma^2}}\right]^{1/2}$$

Particle size distributions from small-angle scattering using global scattering functions, Beaucage, Kammler, Pratsinis J. Appl. Cryst. 37 523-535 (2004).

Particle Size Distribution Curves from SAXS

PDI/Maximum Entropy/TEM Counting

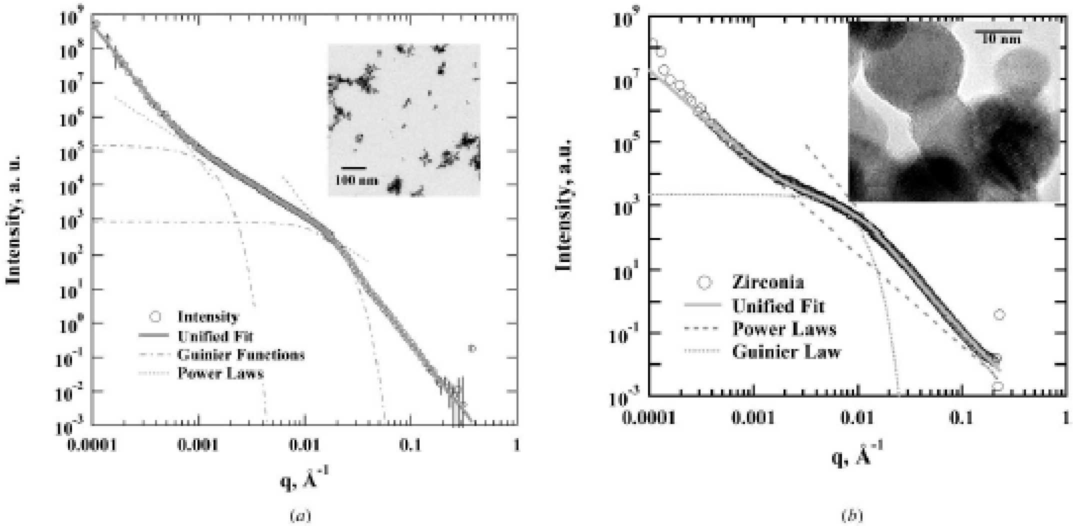

Figure 2
USAXS data from aggregated nanoparticles (circles) showing unified fits (bold grey lines), primary particle Guinier and Porod functions at high q, the intermediate mass fractal scaling regime and the aggregate Guinier regime (dashed lines). (*a*) Fumed titania sample with multi-grain particles and low-q excess scattering due to soft agglomerates. d_{VIS} = 16.7 nm (corrected to 18.0 nm), PDI = 3.01 (σ_g = 1.35), R_g = 11.2 nm, d_f = 1.99, $z_{2:1}$ = 175, z_{R_g} = 226, R_{g2} = 171 nm. From gas adsorption, d_p = 16.2 nm. (*b*) Fumed zirconia sample (Mueller *et al.*, 2004) with single-grain particles, as shown in the inset. The primary particles for this sample have high polydispersity leading to the observed hump near the primary particle scattering regime. d_{VIS} = 20.3 nm, PDI = 10.8 (σ_g = 1.56), R_g = 26.5 nm, d_f = 2.90. From gas adsorption, d_p = 19.7 nm.

Particle size distributions from small-angle scattering using global scattering functions, Beaucage, Kammler, Pratsinis J. Appl. Cryst. 37 523-535 (2004).

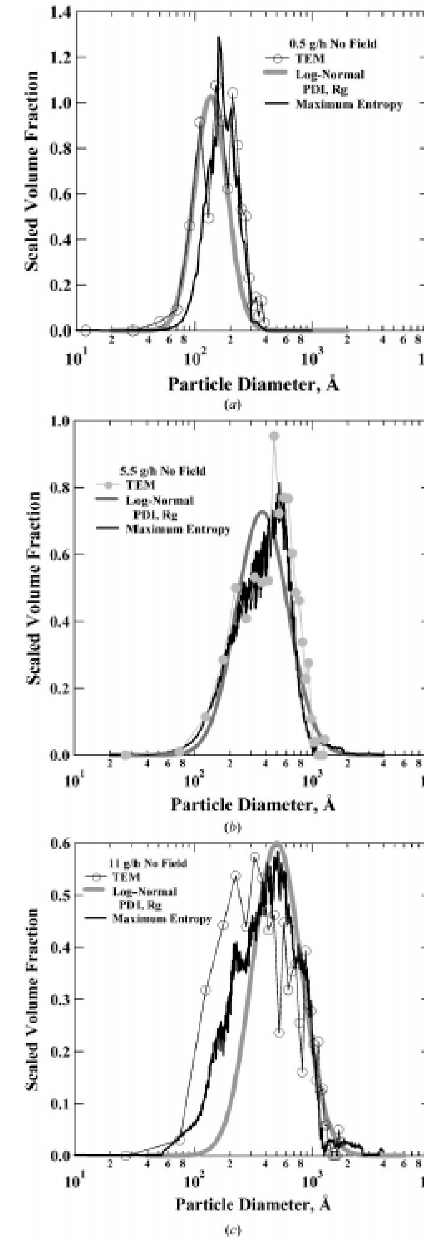

Figure 6
Comparison of particle volume distributions for titania made without an electric field using TEM (circles; Kammler *et al.*, 2003), PDI (grey line) and maximum entropy (black line). (*a*) 0.5 g h^{-1} [fractal d_{VIS} = 12.1 nm, PDI = 3.52 (σ_g = 1.38), R_g = 8.9 nm, d_f = 1.59, $z_{2:1}$ = 1160, z_{R_g} = 1343]. (*b*) 5.5 g h^{-1} [d_{VIS} = 37.2 nm, PDI = 20.0 (σ_g = 1.65), R_g = 50.8 nm]. (*c*) 11 g h^{-1} [d_{VIS} = 46.8 nm, PDI = 15.5 (σ_g = 1.61), R_g = 60.8 nm]. (3 g h^{-1} is shown in Fig. 5.)

Particle Size, d_p

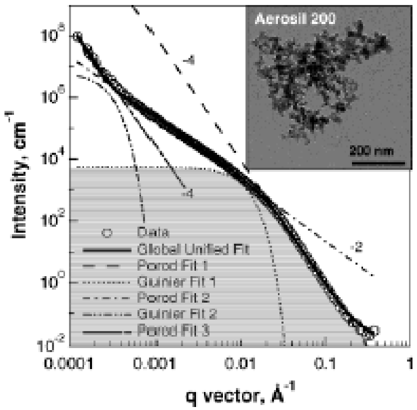

Figure 1. An USAXS pattern of agglomerated fumed silica (Aerosil 200, Degussa AG). The scattering data (circles) are well described by the global unified fit equation (solid line). Furthermore, three Porod regimes (dashed line, dashed−dotted line, and long−short-dashed line) are shown together with the Guinier regimes (dotted line and dashed−double-dotted line). The appearance of the second Porod (weak power-law) regime (0.0005 Å^{-1} < q < 0.01 Å^{-1}) proves that these particles are agglomerated and mass fractal as shown by the TEM insert. The gray shaded area indicates the integral part for determination of d_{VS}.

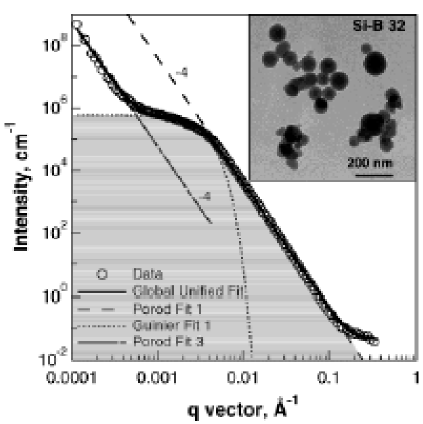

Figure 2. A USAXS plot of a nonagglomerated fumed silica (Si-B 32) made in a 17 g/h sustained premixed flame reactor (ref 18). The scattering data (circles) are well described by the global unified fit equation (solid line). Furthermore, Porod regimes (dashed line and long−short-dashed line) are shown together with the Guinier regime (dotted line). The lack of the Porod (weak power-law) regime at 0.0005 Å^{-1} < q < 0.005 Å^{-1} indicates that the particles are nonagglomerated as shown by the TEM insert. The gray shaded area indicates the integral part for determination of d_{VS}.

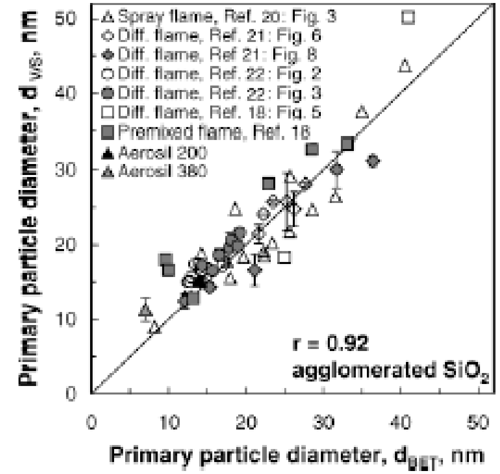

Figure 3. Comparison of d_{VS} and d_{BET} for agglomerated silica powders made in our vapor- or liquid-fed flame aerosol reactors (refs 18 and 20−22) and those of commercially available powders (Aerosil 200 and Aerosil 380, Degussa AG).

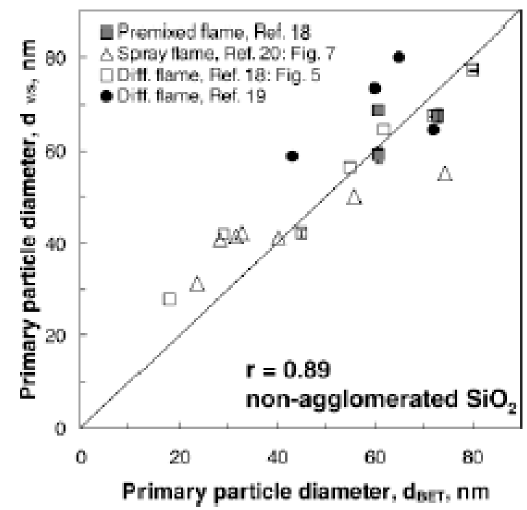

Figure 4. Comparison of d_{VS} and d_{BET} for various nonagglomerated silica powders made in our vapor-fed (refs 18 and 19) and liquid-fed (ref 20) flame aerosol reactors.

Structure of flame made silica nanoparticles by ultra-snall-angle x-ray scattering. Kammmler HK, Beaucage G, Mueller R, Pratsinis SE *Langmuir* **20** 1915-1921 (2004).

Polydisperse Particles

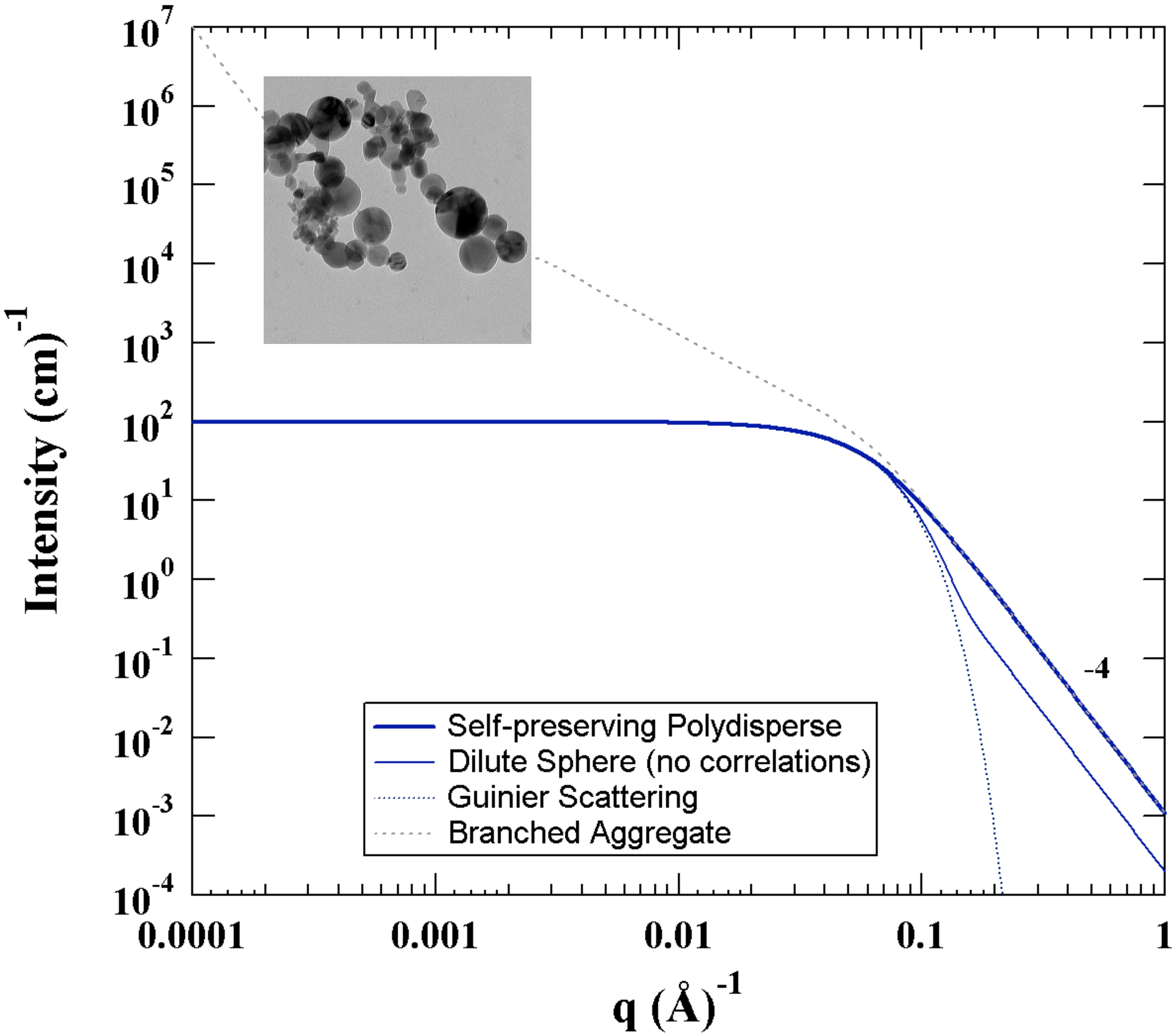

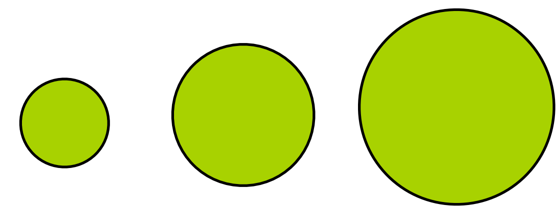

$$PDI = \frac{B_P R_g^4}{1.62G}$$

$$\sigma = \ln(\sigma_g) = \left[\frac{\ln(PDI)}{12}\right]^{1/2}$$

$$m = \left[\frac{5R_g^2}{3e^{14\sigma^2}}\right]^{1/2}$$

Particle size distributions from small-angle scattering using global scattering functions, Beaucage, Kammler, Pratsinis J. Appl. Cryst. 37 523-535 (2004).

Linear Aggregates

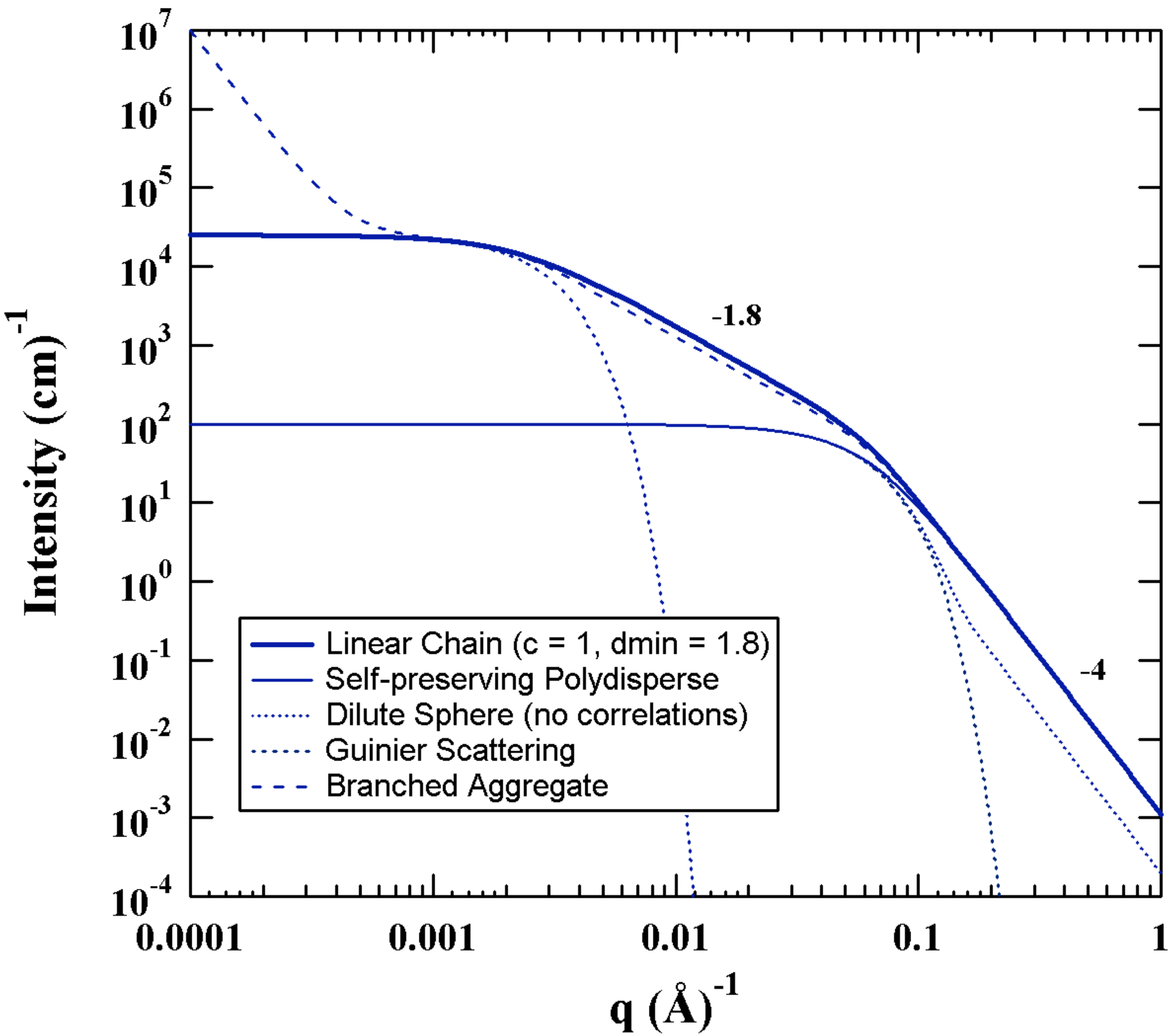

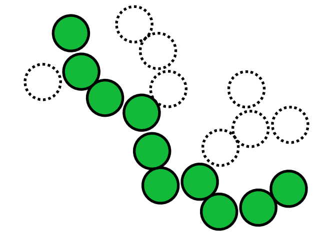

$$I(q) = G_2 \exp\left(\frac{-q^2\left\langle R_{g,2}^2\right\rangle}{3}\right)$$

$$z = \frac{G_2}{G_1} = \left(\frac{R_2}{R_1}\right)^{d_f}$$

$$I(q) = B_f q^{-d_f}$$

$$B_f = \frac{G_2 d_f}{R_{g,2}^{d_f}} \Gamma\left(d_f/2\right)$$

Beaucage G, Small-angle Scattering from Polymeric Mass Fractals of Arbitrary Mass-Fractal Dimension, J. Appl. Cryst. 29 134-146 (1996).

Branched Aggregates

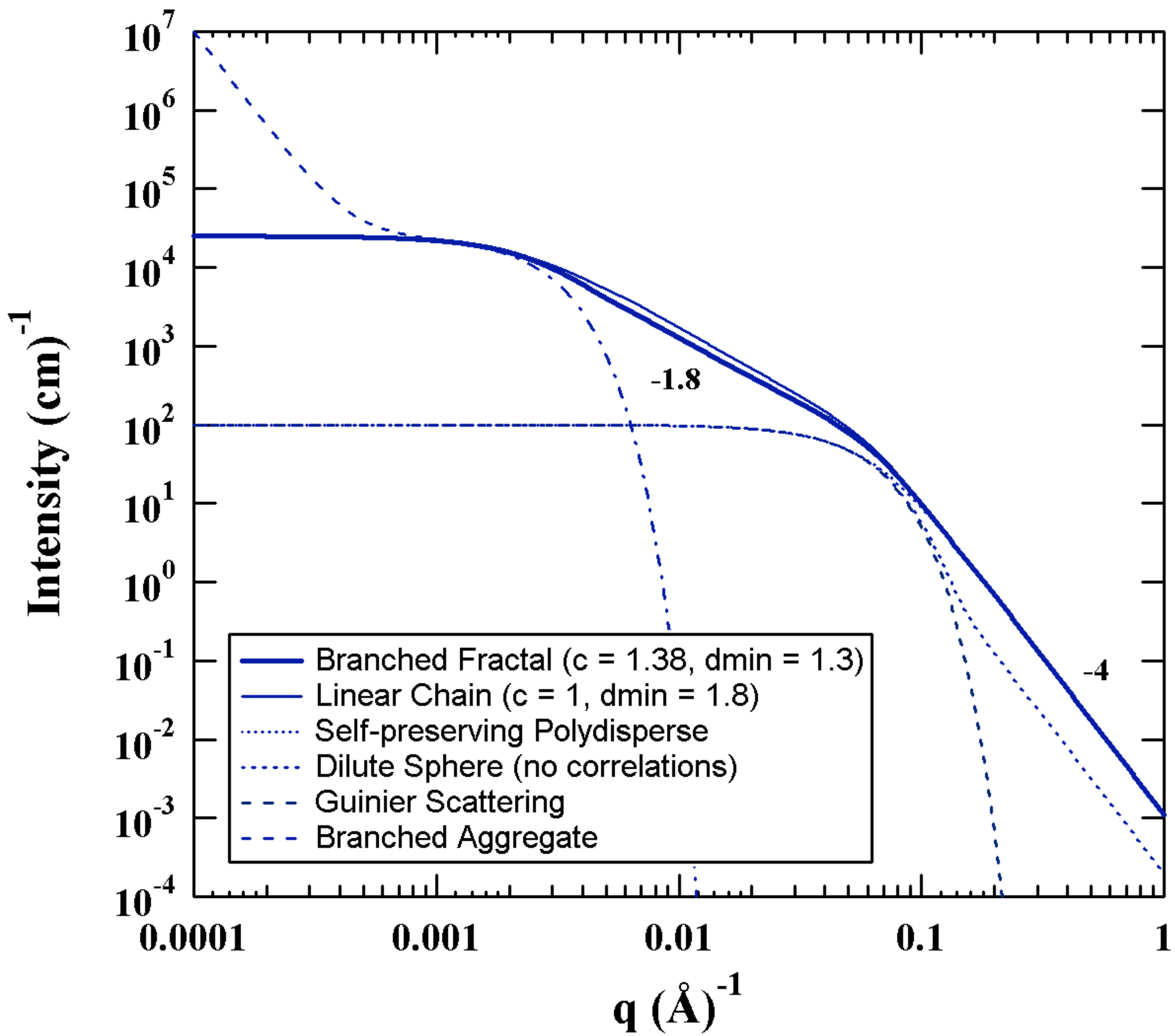

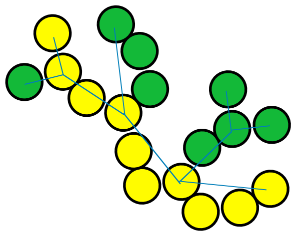

$$z = p^c = s^{d_{\min}}$$

$$d_f = c d_{\min}$$

$$\phi_{Br} = \frac{z - p}{z} = 1 - z^{1/c - 1}$$

$$B_f = \frac{G_2 d_{\min}}{R_{g,2}^{d_f}} \Gamma\left(d_f / 2\right)$$

Beaucage G, Determination of branch fraction and minimum dimension of fractal aggregates Phys. Rev. E 70 031401 (2004).

Large Scale (low-q) Agglomerates

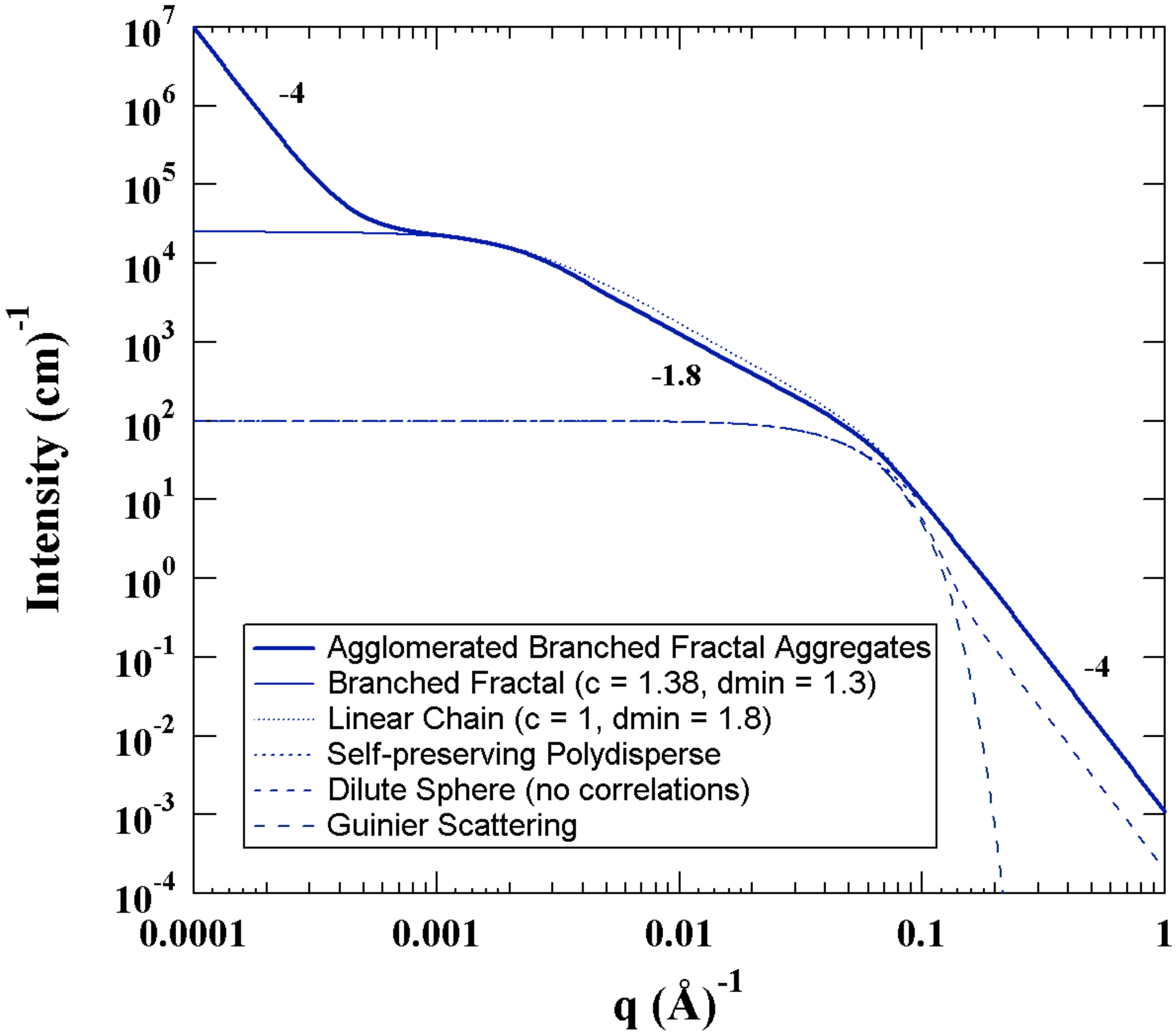

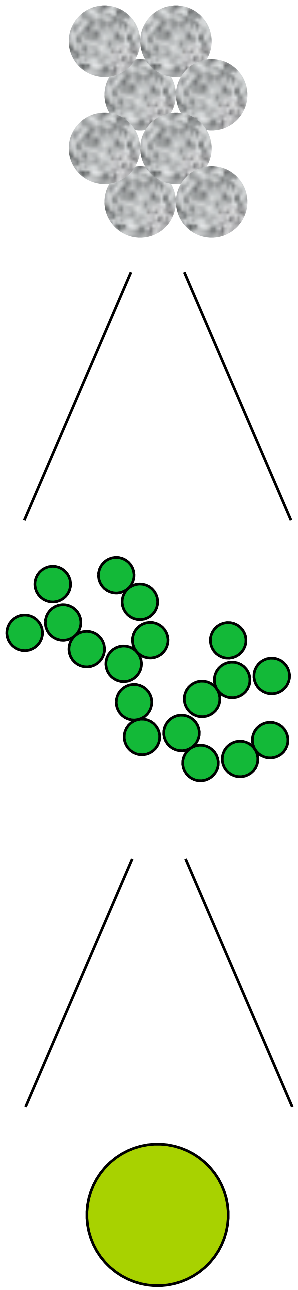

$$I(q) = B_P q^{-4}$$

Small-scale Crystallographic Structure

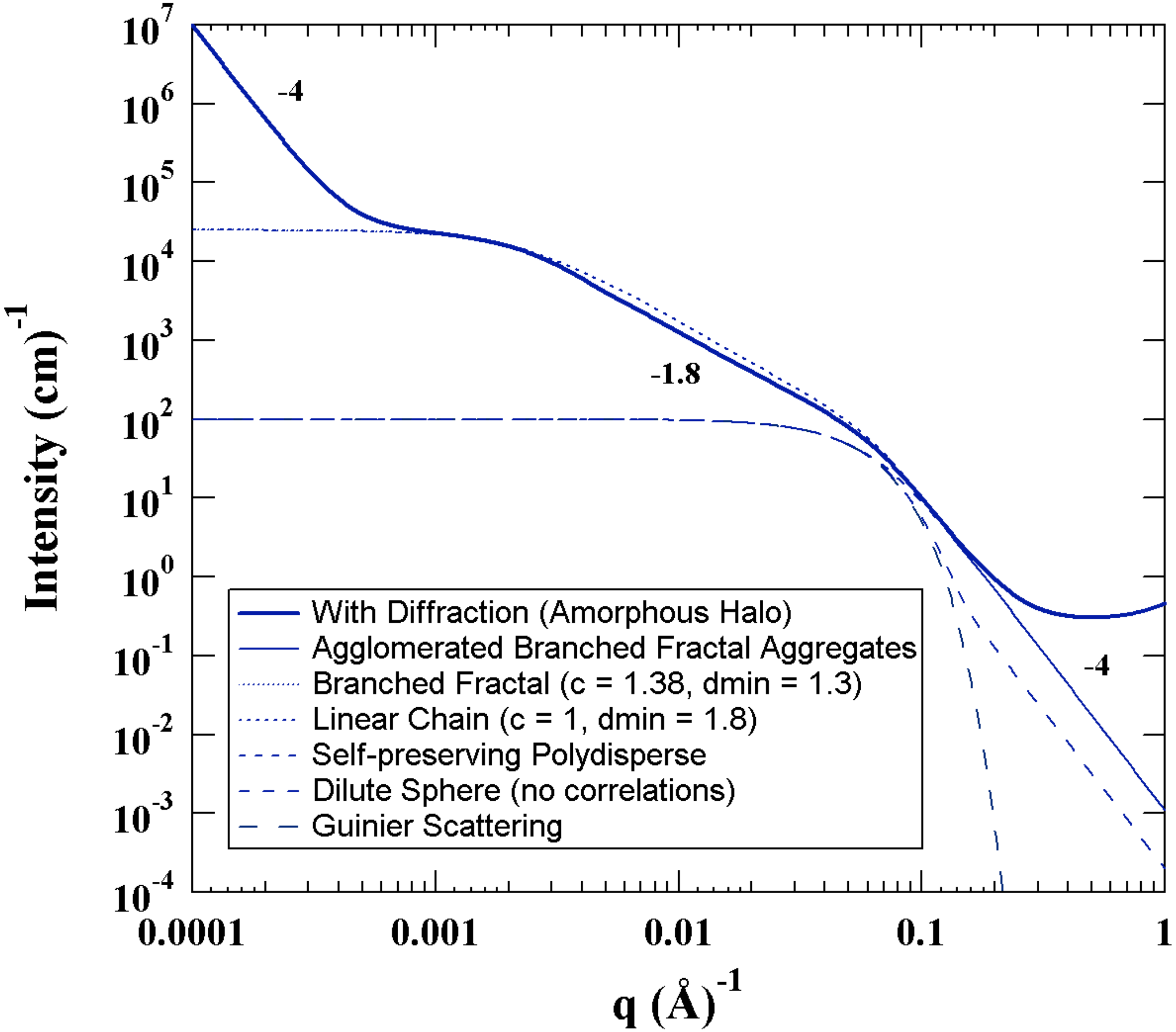

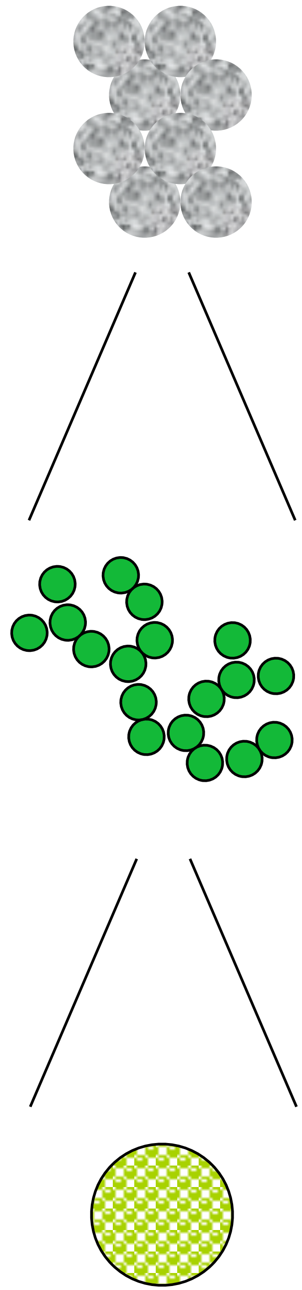

Branched Aggregates

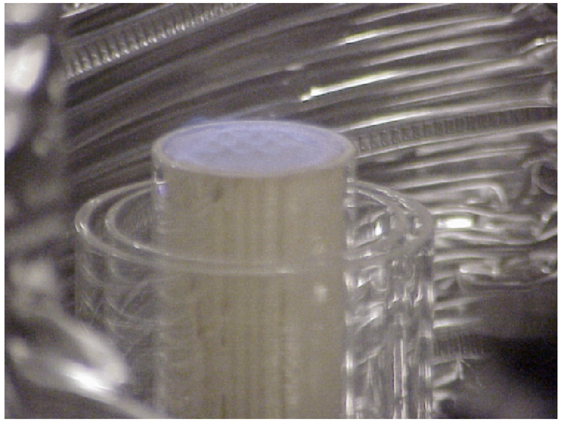

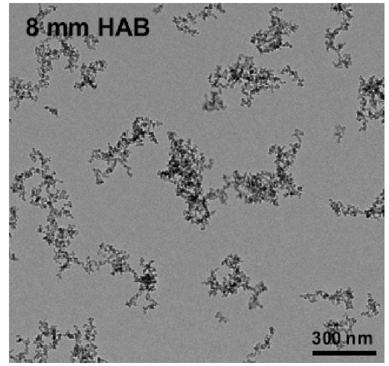

APS UNICAT
Silica Premixed Flames
J. Appl. Phys 97 054309 Feb 2005

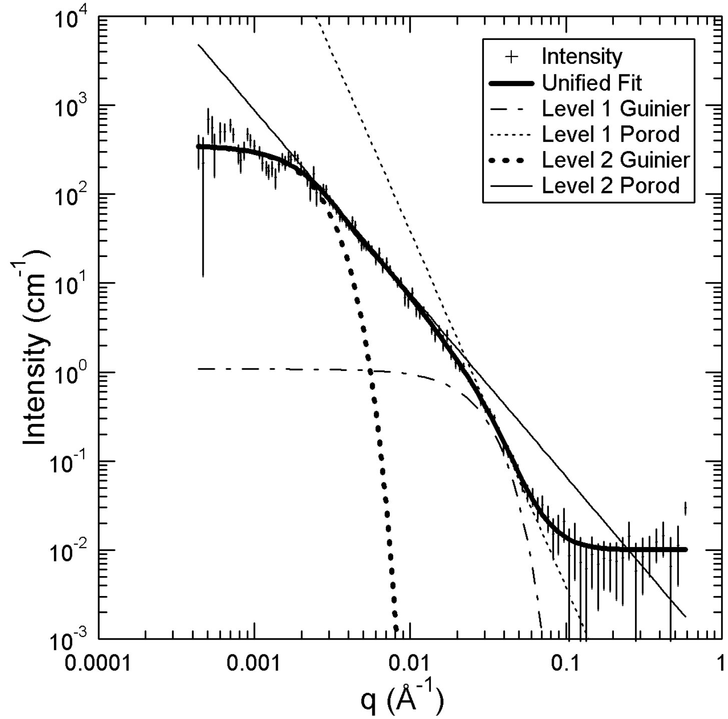

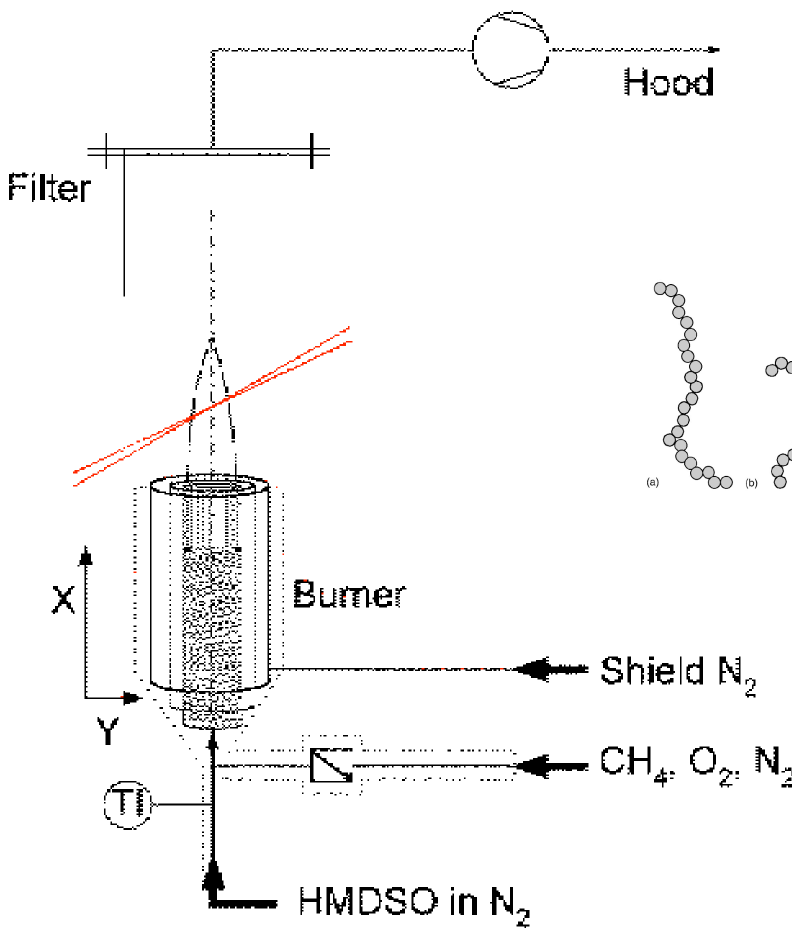

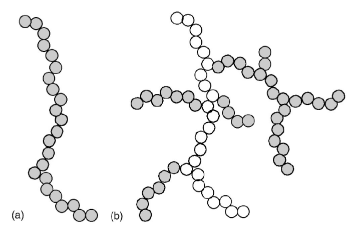

5mm LAT 16mm HAB
Typical Branched Aggregate
$d_p = 5.7$ nm
$z = 350$
$c = 1.5$, $d_{min} = 1.4$, $d_f = 2.1$
$\phi_{br} = 0.8$

Beaucage G, *Determination of branch fraction and minimum dimension of fractal aggregates* Phys. Rev. E 70 031401 (2004).

Examples of Application to In Situ Studies of Flame Made Nanoparticles

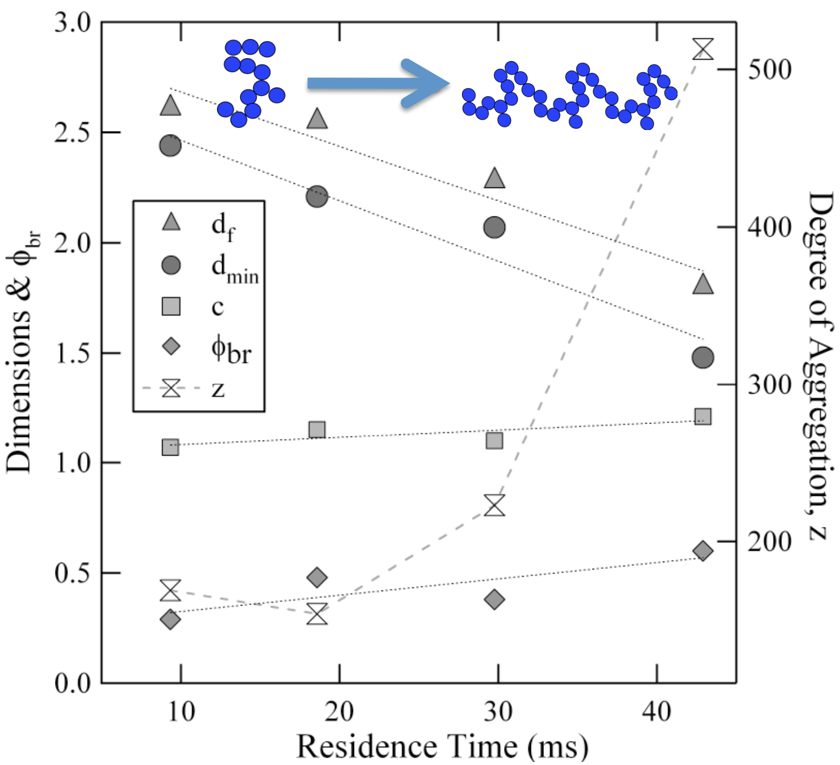

Sztucki M, Narayanan T, Beaucage G, *In situ study of aggregation of soot particles in an acetylene flame by small-angle x-ray scattering* J. Appl. Phys. **101**, 114303 (2007).

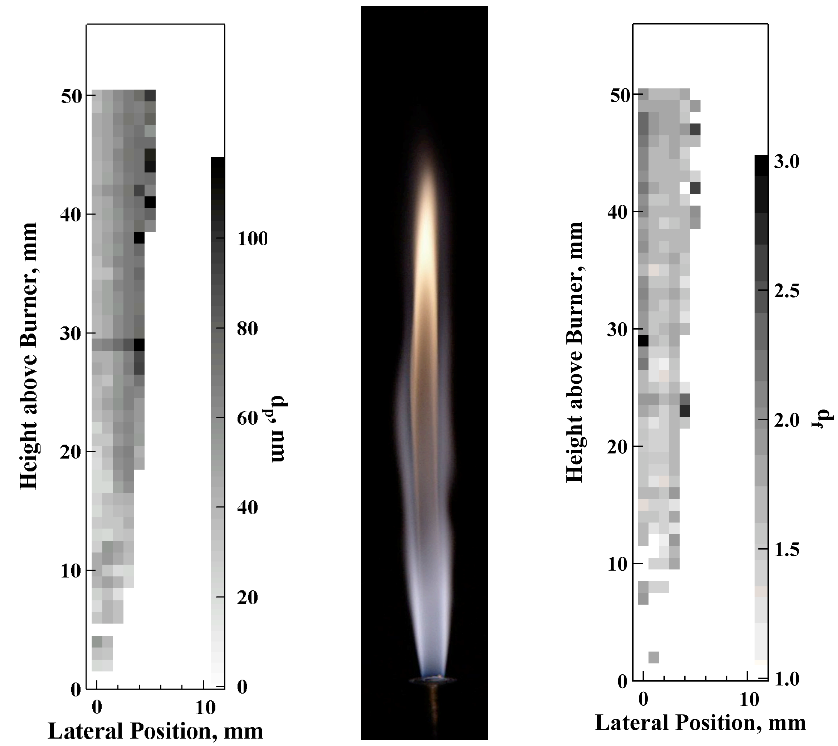

Kammler HK, Beaucage G, Kohls DJ, Agashe N. Ilavsky J *J Appl. Phys.* **97**(2005) (Article 054309).

Beaucage, G., H. K. Kammler, S. E. Pratsinis, T. Narayanan... *Probing the dynamics of nanoparticle growth in a flame using synchrotron radiation. Nature Mater.*, **3**, 370-373 (2004).

SAXS and DMA Comparison

Typical Diesel Particle Size Distributions, Number, Surface Area, and Mass Weightings Are Shown

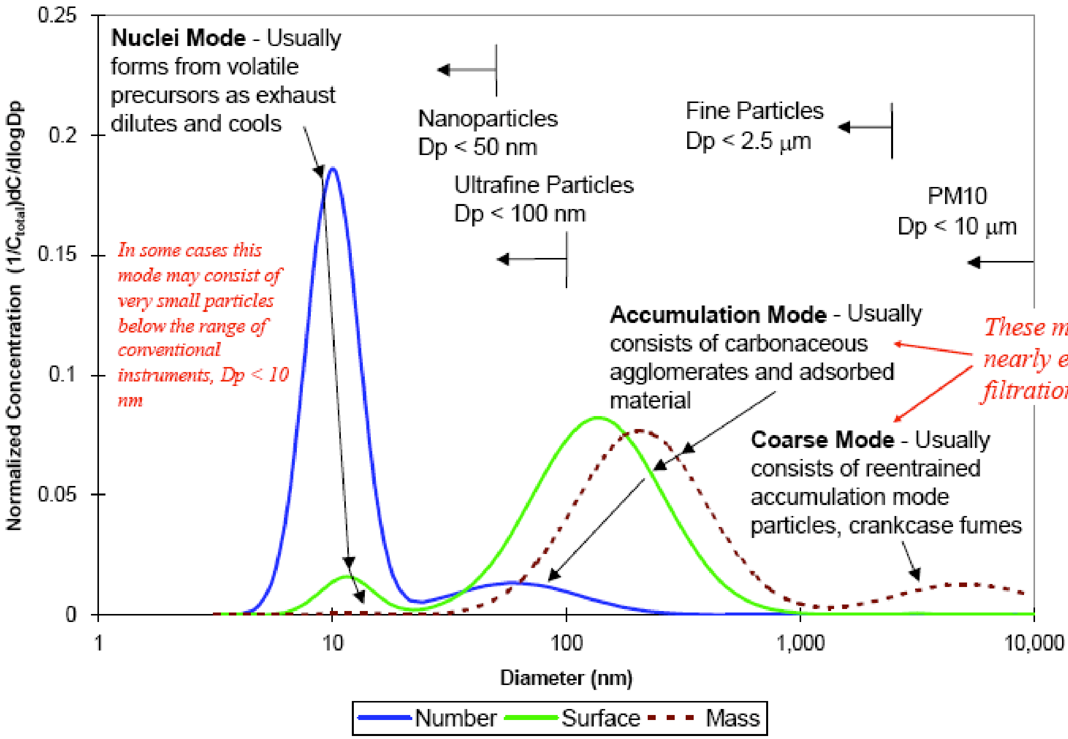

Engines and Nanoparticles a Review, Kittelson DA, *J. Aerosol Sci.* **29** 575-588 (1998) as modified in a talk online.

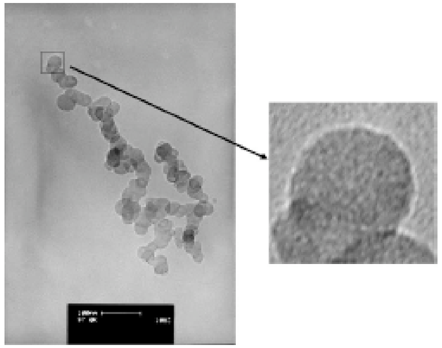

Fig. 1. Diesel soot agglomerate composed of spherical primary particles.

Lapuerta M, Ballesteros R, Martos FJ, *J. Col. And Interf. Sci.* ***303****, 149-158 (2006).*

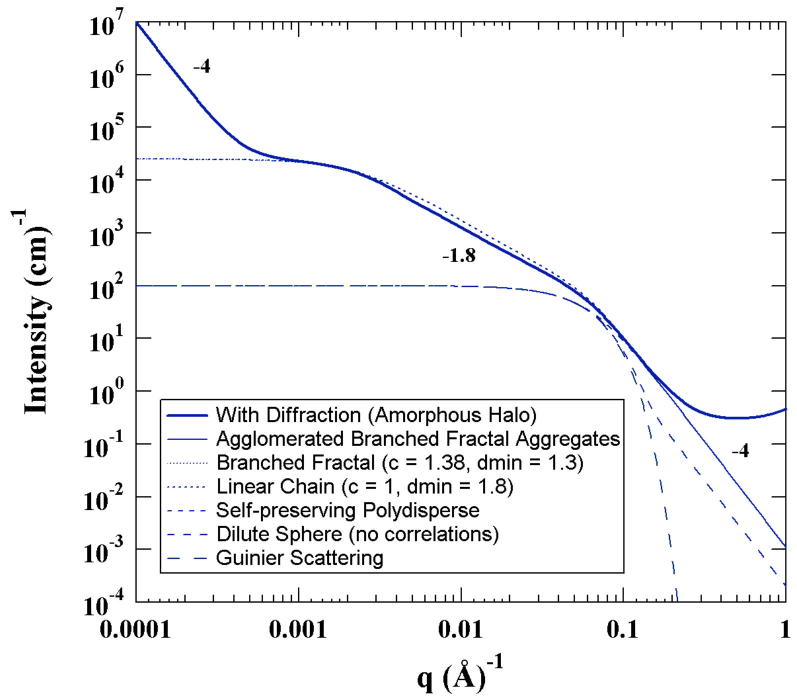

Experimental Setup for in situ Exhaust SAXS Measurement

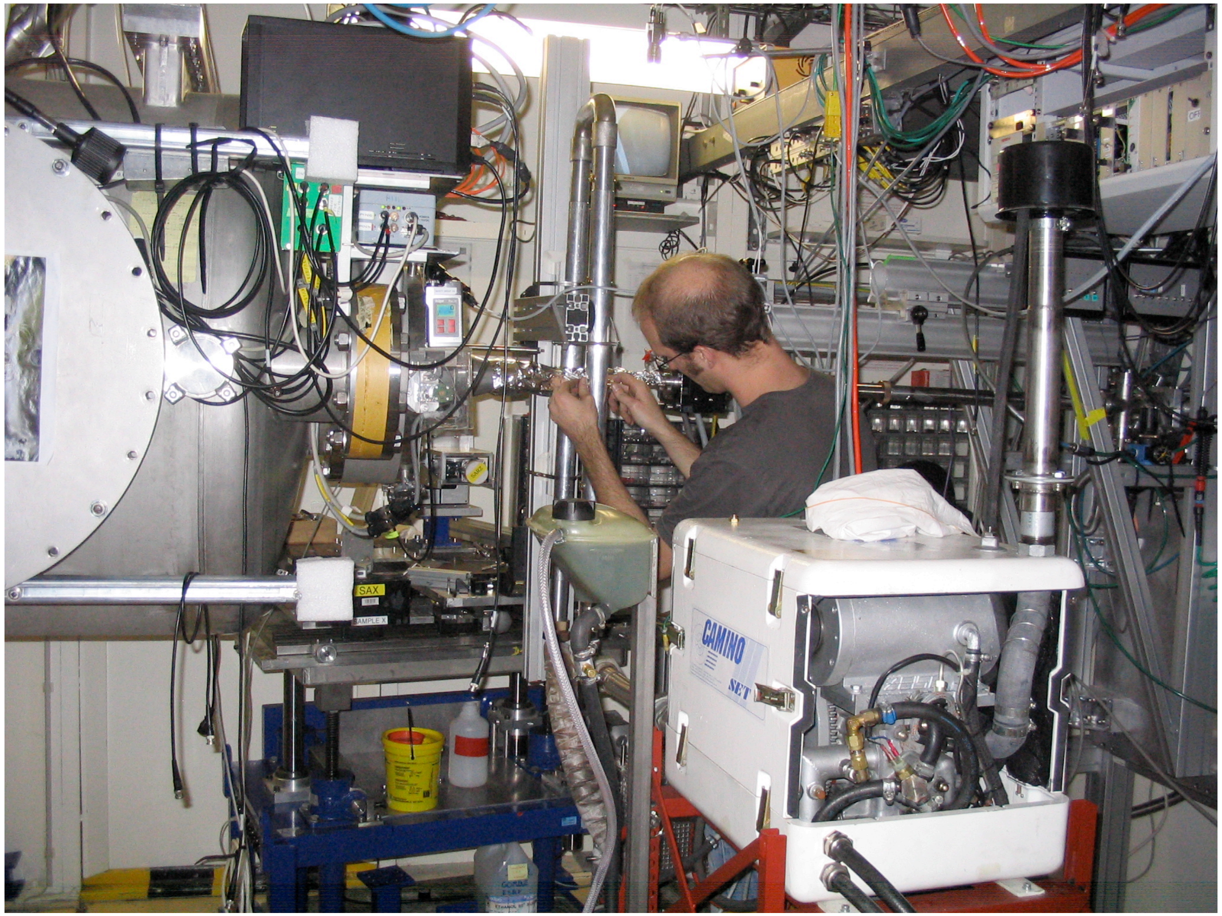

<u>Camino Generator Set</u>
4- Stroke Direct Injection
Water Cooled
Single Cylinder
Bore: 65 mm, Stroke: 62 mm
210 cc displacement
2.95 kW
2,600 RPM (Constant)
No Turbocharger
Fixed Fuel Feed Rate
Exhaust Temperature 271-194 °C
Vary Load Using Water Heater
Measure 1.5 m in Steel Exhaust Pipe

<u>We consider here two fuels</u>

1) "Regular" Diesel (UN 1202)
   - Centane Number 43
   - Sulfur <10.0 mg/kg
   - ρ = 829 kg/m^3; η /ρ = 2.33 mm^2/s at 40°C
   - Boiling Point 336 °C
2) Kerosene
   - Centane Number 51
   - Sulfur 9.5 mg/kg
   - ρ = 776 kg/m^3; η/ρ = 1.07 mm^2/s at 40°C
   - Boiling Point 226 °C

The Influence of additives on the size distribution and composition of particles produced by diesel engines. Skillas G, Qian Z, Baltensperger U, Matter U & Burtscher H, *Combust. Sci. and Tech.* **154** 159-273 (2000). & Skillas G Dissertation ETHZ (1999) *Carbon Nanostructures from Combustion: Morphology, Density and Applications.*

Similar to generator set used by:
Rethinking Organic Aerosols: Semivolatile Emissions and Photochemical Aging, Robinson AL, Pandis SN et al. *Science* **315** 1259-1262 (2007).

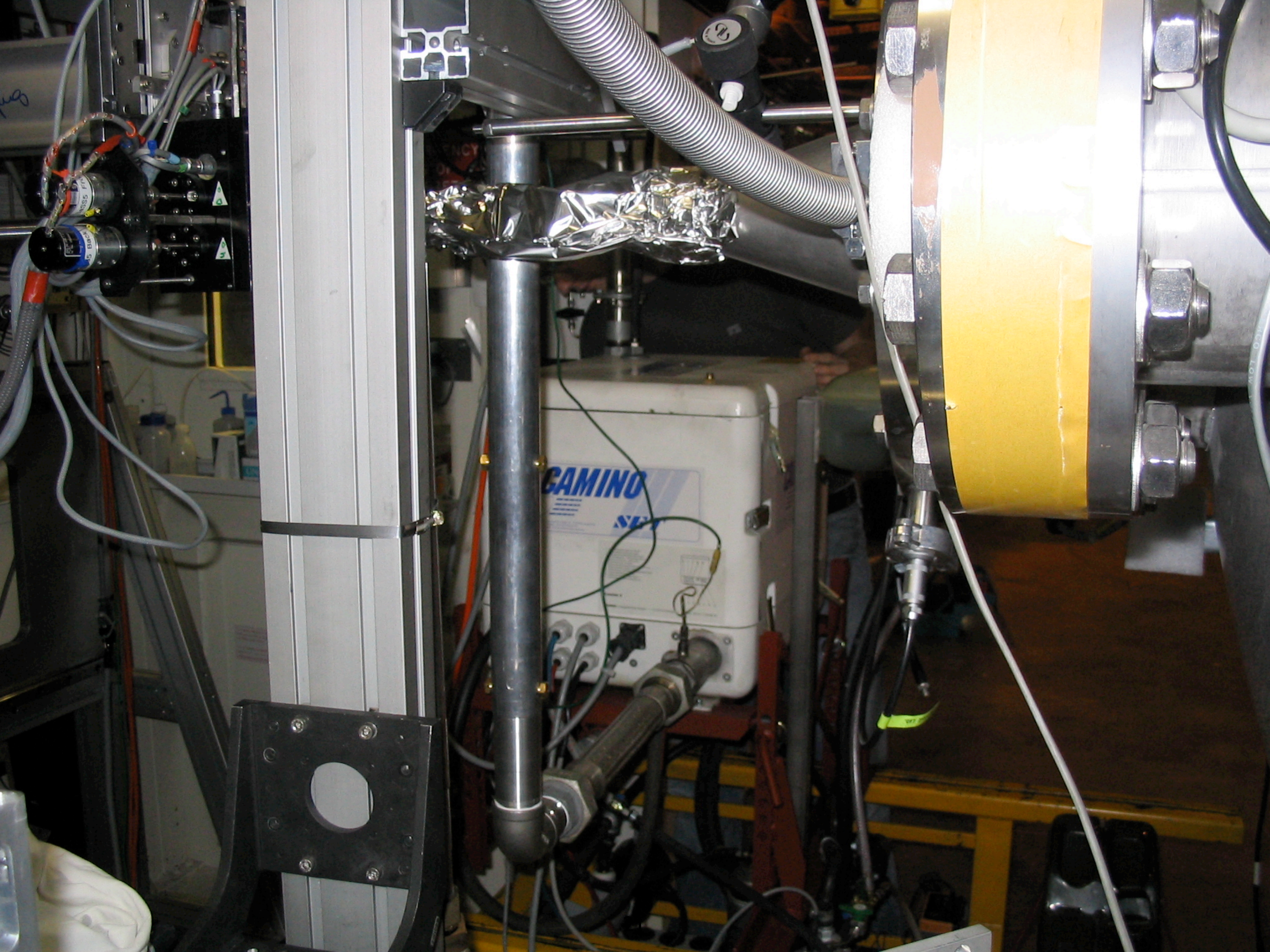
CAMINO

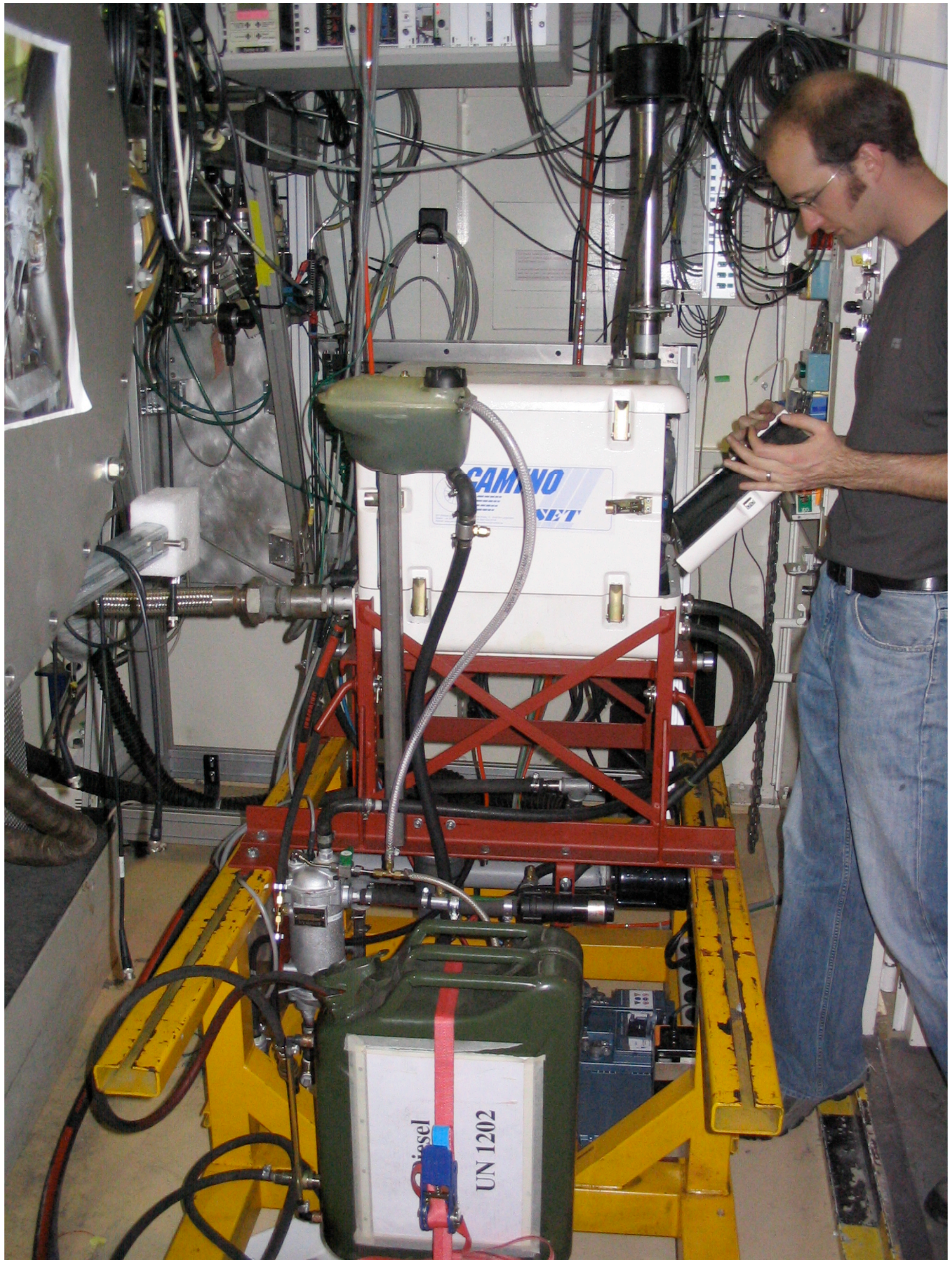

Diesel
UN 1202

Merci
de
fermer
la porte
ID02

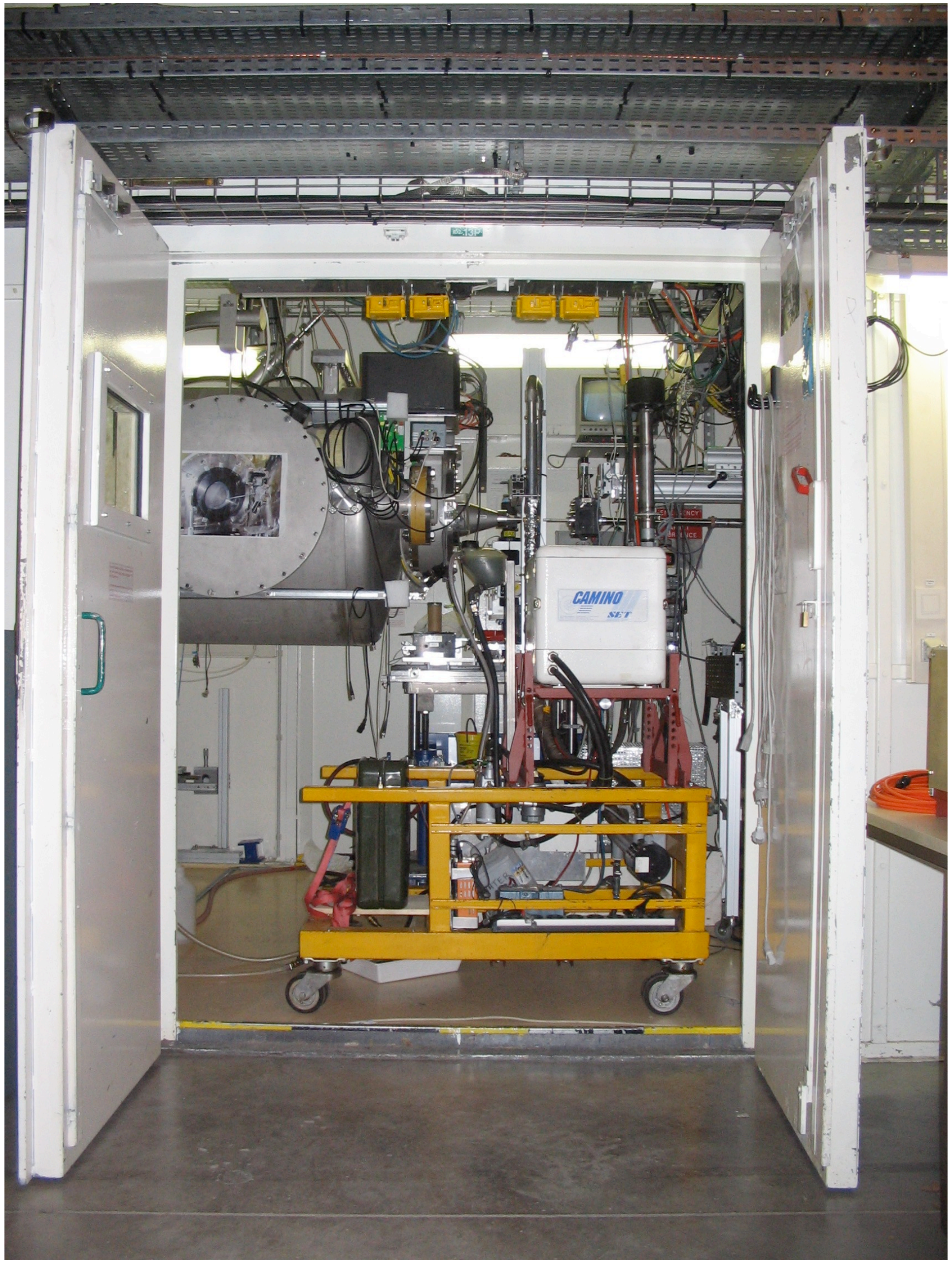
CAMINO
SET

In Situ Exhaust Measurement
20 ms Exposure on Exhaust Stream

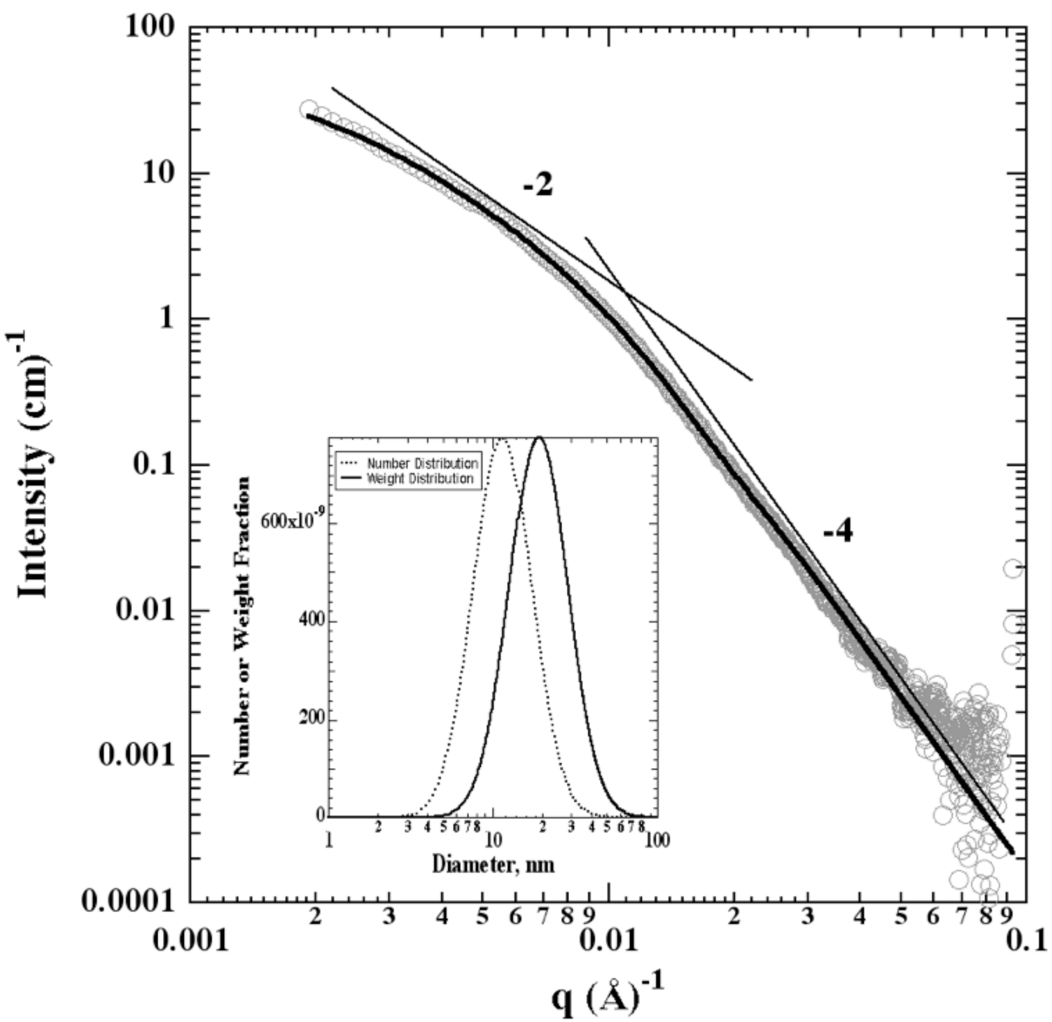

d_p = 19.2 nm
σ_g = 1.48 (PDI = 6.40)
d_f = 2.10, c= 1.03
z = 43.6
ϕ_{Br} = 0.104

Startup Regular Diesel

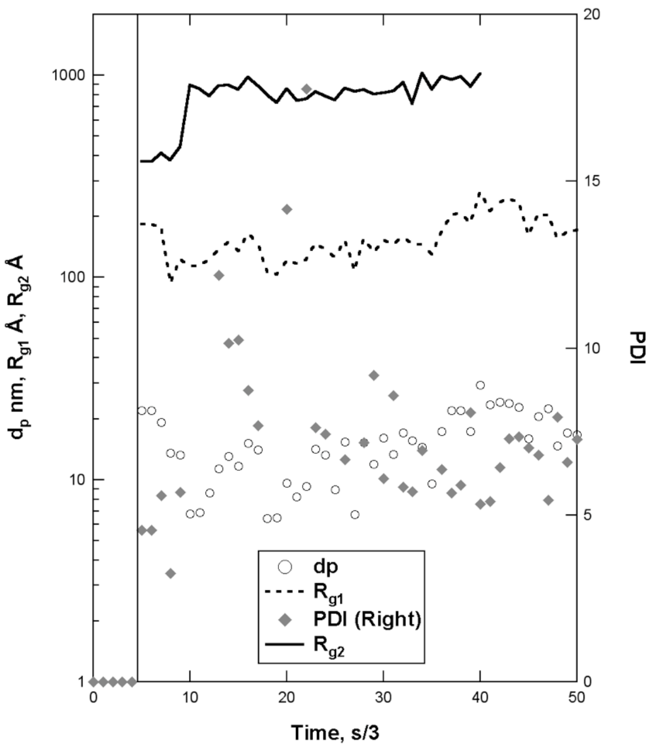

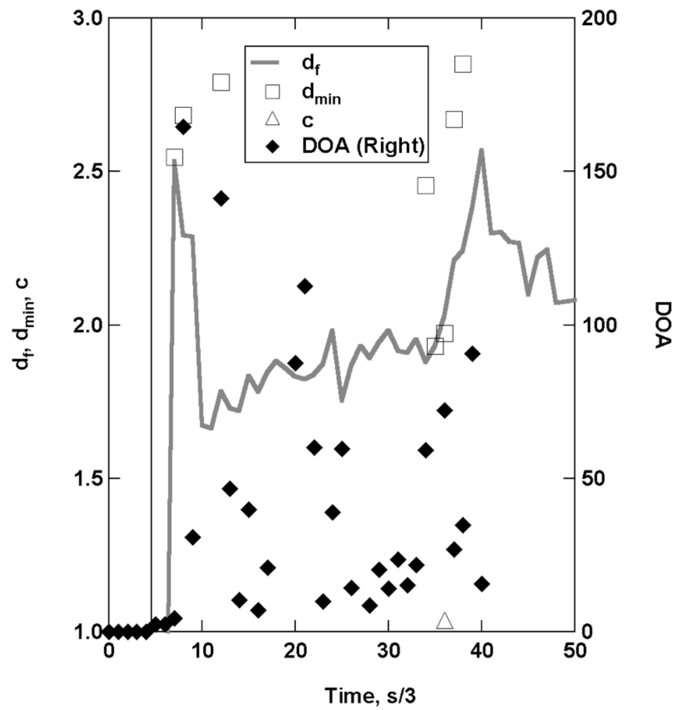

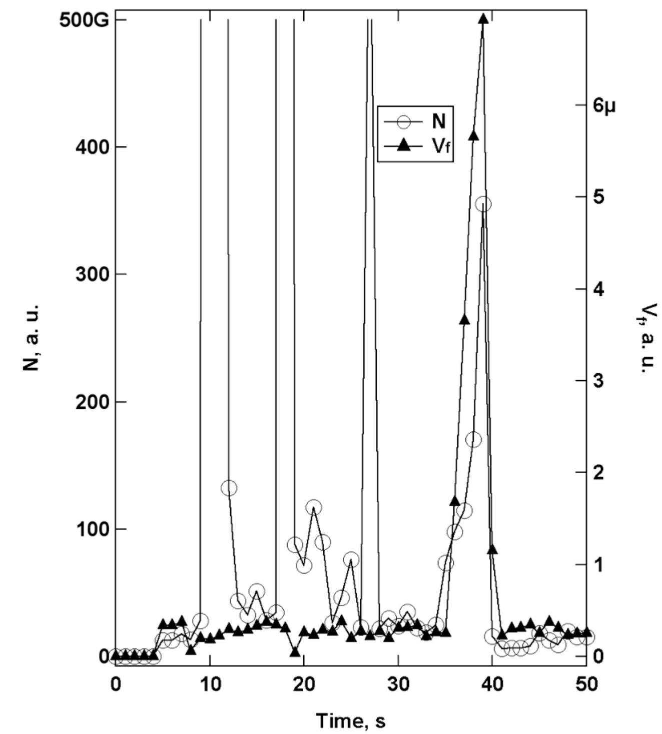

Startup Kerosene

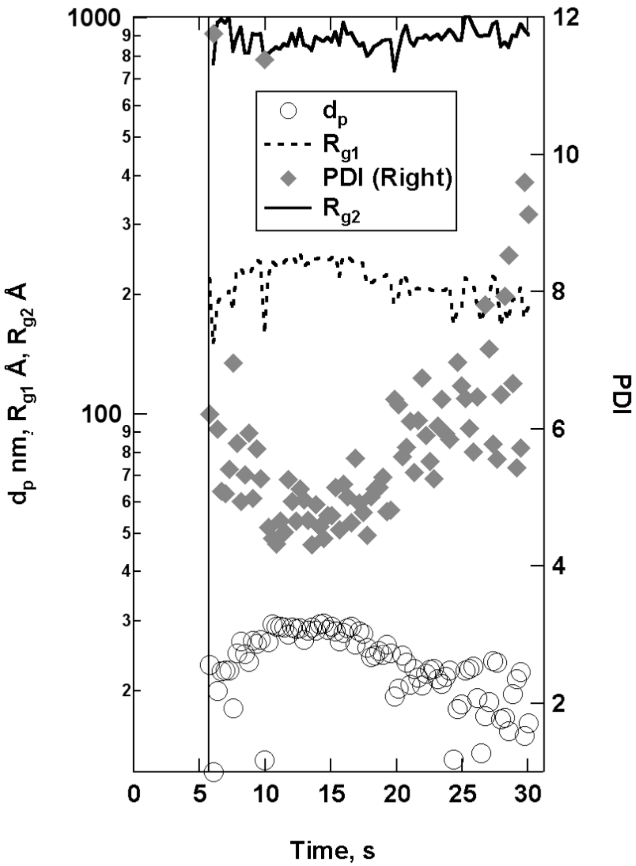

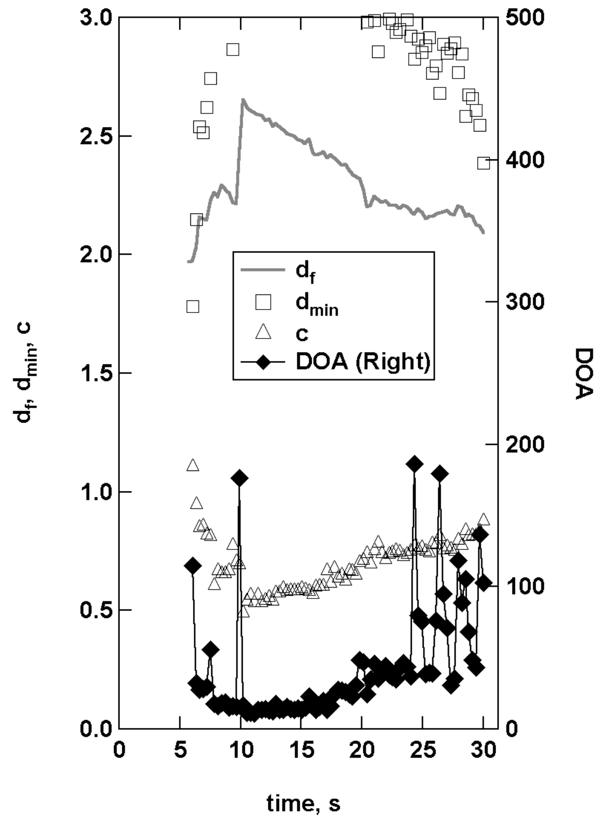

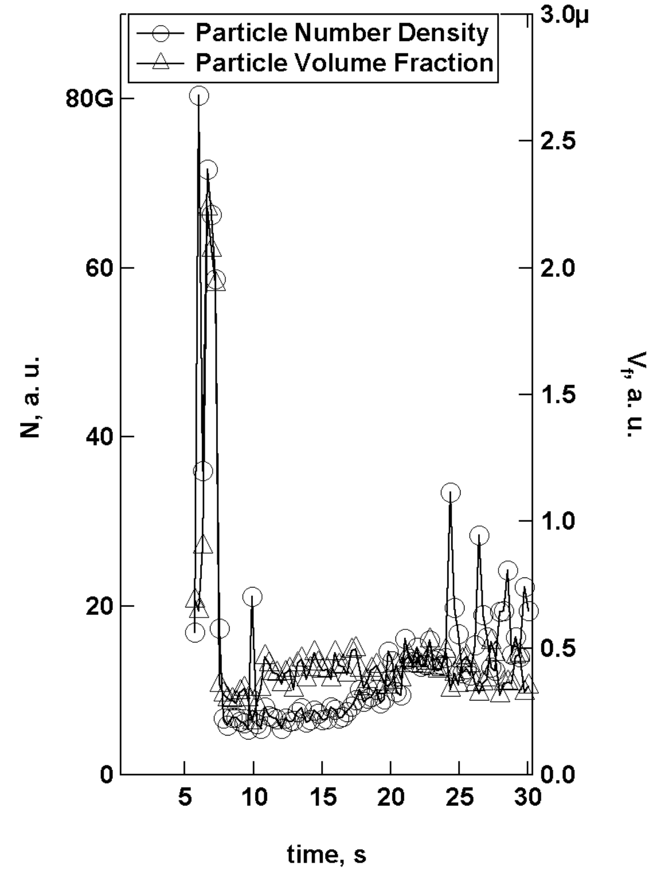

Full Load Removed Regular Diesel at 12 s

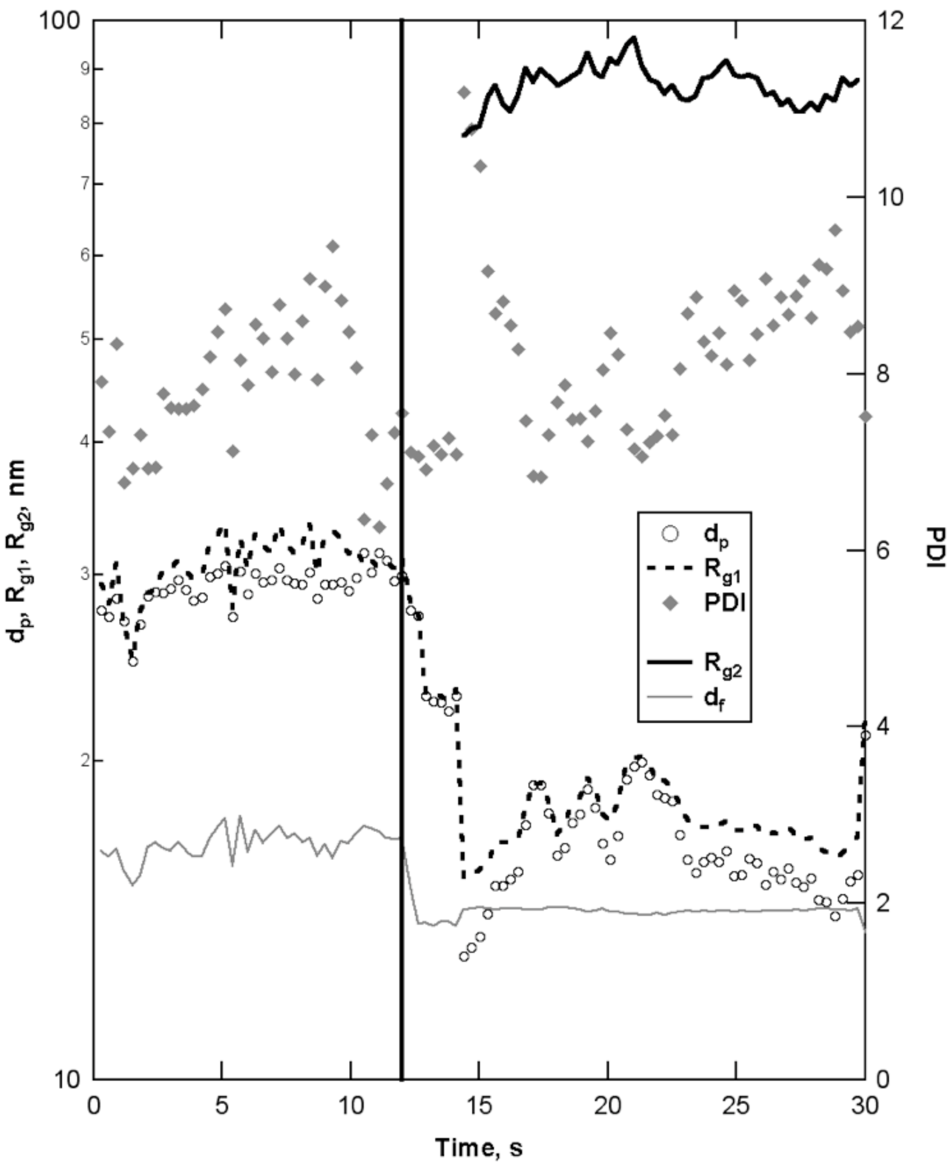

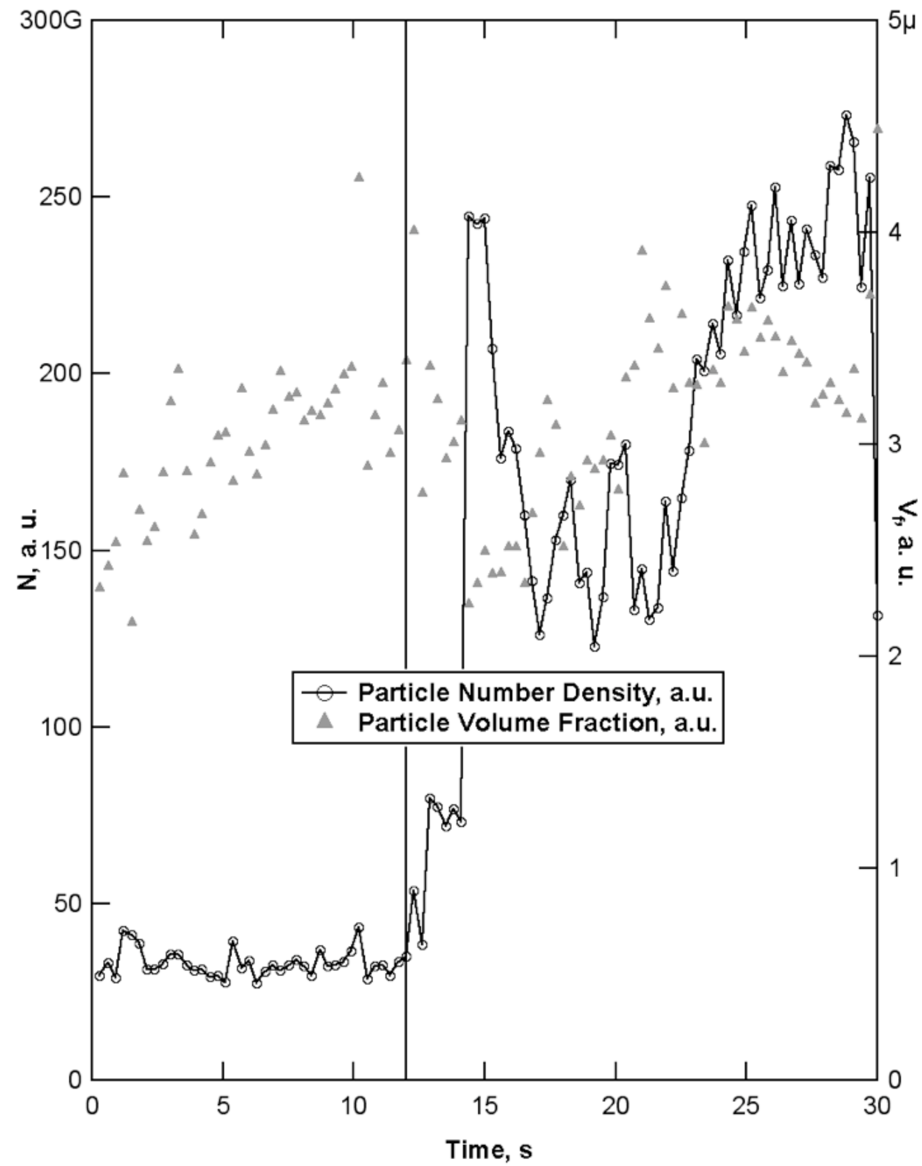

Why you might be interested in SAXS:

-In situ observation of soot & inorganic nanostructure with no dilution
(calibrate/verify DMA)
-Measure from ~ 1 Å to 1 μm (direct observation of all possible nucleation modes)
-Wide sample concentration range solid powder to exhaust aerosol
-Volatile, semi-volatile, and solid particles (no dilution, charging or denuding)
-Unique details of aggregate structure including mass fractal dimension, branch content
-Volume and number density as well as primary particle size distribution
-20 ms measurement (possibility of observation within engine cycle)

Why you might *not* be interested in SAXS

-Requires a synchrotron for in situ aerosol measurements
(powders can be measured in the lab)
-Non-portable measurement
-More or less requires a specialist (involved data anaylsis)
-Composition is more difficult than structure (electron density or use anomalous SAXS)
-New method (This is the pioneering study and is still in preparation for publication)

Supported by "*misdirected*" funds from US NSF (CBET); The Swiss National Science Foundation; ESRF and related EU funding; The Aerothermochemistry and Combustion Systems Laboratory at ETH and the inquisitive interest of K. Boulouchos and P. Kirchen at ETH and T. Narayanan at ESRF.

	Reference	Fuel 2
Density (kg/m^3):	829	776
Evaporation Temperature (°C)	336	226
Cetane Number (-)	51	43
Sulfur Content (mg/kg)	9.5	< 10.0
Aromatic Content (Mass %)	18.6	1.9
Viscosity (mm^2/s at 40°C)	2.33	1.07